

4. Geochemical study of the Bakening volcano and surrounding monogenetic centers

Frank Dorendorf ¹, Tatiana Churikova ², Alexander Koloskov ² and Gerhard Wörner ¹

¹ Geochemisches Institut, University of Göttingen, Goldschmidtstr. 1, 37077 Göttingen, Germany

² Institute of Volcanology and Geochemistry FED RAN, Piip Avenue 9, Petropavlovsk-Kamchatsky, Russia

Abstract

Major and trace elements as well as isotopes have been studied at Bakening volcano (Kamchatka) and contemporaneous basaltic monogenetic centers to assess the different roles of variable mantle sources and intra-crustal differentiation processes.

Three main suites of volcanic activity are recognized in the area: (1) plateau basalts of Lower Pleistocene age, (2) andesites and dacites of the Bakening volcano, the New Bakening volcano dacitic centers nearby, and (3) contemporaneous basaltic cinder cones erupted along subduction zone - parallel N-S faults. New age-data of Dirksen and Melekestsev (1998) show that the last eruptions in the Bakening area occurred only 600-1200 a ago, suggesting the volcano as potentially active.

Major element variations and petrographic observations provides evidence for a fractionation assemblage of olivine, clinopyroxene, \pm plagioclase, \pm magnetite(?) within the basaltic suite. The fractionation in the andesites and dacites is dominated by amphibole, clinopyroxene, orthopyroxene and plagioclase plus minor amounts of magnetite and apatite. The youngest cpx-opx-andesites of Bakening main volcano deviate from that trend. Their source was probably formed by mixing of basaltic magmas into the silicic magma chamber of the Bakening volcano. Overall trace element patterns as well as the Sr-Nd-Pb isotopic compositions are quite similar in all rocks despite large differences in their chemical composition (from basalt to rhyodacite). In detail however, the andesite-dacites of the central Bakening volcano show a stronger enrichment in the more incompatible elements and depletion in HREE compared to the monogenetic basaltic centers. This results in a crossing of

the REE-pattern for the two suites. The decrease in the REE's can be explained with high-P amphibole fractionation. However the higher relative amounts of LILE in the dacitic and the large scatter in the basaltic rocks must be the result of variable source enrichment by slab-derived fluids overprinting a variable depleted mantle wedge. The plateau basalts are probably derived from a mixture of DM and EM sources.

Introduction

Active arc volcanism on Kamchatka comprises from E to W three major zones : (1) the Eastern volcanic front (EVF), (2) the Central Kamchatka depression with the famous Kluchevskaya Group (CKD), and (3) the western volcanic chain of the Sredinny range (SR). The Late Pleistocene to Holocene Bakening volcano is situated 100 km to the North of Petropavlovsk-Kamchatsky at the sources of Srednaya Avacha and Pravaya Kamchatka rivers. It is situated between the CKD and the Eastern volcanic front. The volcanic front 60 km to the E is formed by the Avacha, Koryaksky, Zupanovsky and Semyachik volcanoes.

Bakening basement is formed by Miocene volcano-sedimentary rocks of the Ganalsky ridge. Lower Cretaceous sedimentary rocks and Miocene intrusive rocks are exposed at the uplifted E border of the Srednaya Avacha valley. Lower Quaternary plateau basalts and andesites with an intra-plate signature can be found in the N and SE of Bakening. These rock units are bordered by Lower to Middle Pleistocene N-S directed faults. A maximal vertical displacement of up to 2500m occurred in the Srednaya Avacha depression, there where later the Bakening stratovolcano developed (Zjurupa, 1978). This old fault system is crossed by the NNE-SSW directed Late Pleistocene fault system. These younger faults are obviously connected with the same stress field that also formed the Central Kamchatka Depression.

Quaternary volcanism in the studied area is bimodal. Andesitic to dacitic rocks form the Bakening stratovolcano (2277m) and some adjacent cones nearby. Monogenetic cinder cones are developed at the intersection of the two fault systems and characterized by mainly basaltic volcanism. Both suites erupted closely in space and time.

Recently Bakening volcano received increasing interest, because Dirksen and Melekestsev (1998) proved that most recent eruptions are only about 1200-600 years old, indicating that the Bakening volcano can be regarded as potentially active. Up today the study of Bakening volcano was mainly geomorphologically and petrographically (Melekestsev et al., 1998; Piip,

1947; Svjatlowsky, 1956; Zjurupa, 1978). This paper provides the first modern geochemical investigation of Bakening volcano including its monogenetic centers in the surrounding. We use major and trace elements as well as isotopes, to examine how the volcanism has developed in this region in the Quaternary and find out if the bimodal volcanism is linked with different mantle sources.

Analytical procedures

Major and some trace elements (Ba, Co, Cr, Ga, Ni, Rb, Sc, Sr, V, Y, Zn, Zr) were measured on glass fusion discs by standard XRF analysis. The 2σ -error for major elements is lower than 1 % (except FeO and Na₂O with 2 %), for trace elements lower than 5 % (until the limit of 20-30 ppm). The error of determination of the LOI (lost of ignition) is around 10 %. All other trace elements were determined by ICPMS. Errors (2σ) of this method in the time of this study were lower than 20 % for Nb and Ta, lower than 10 % for Be, Cs, Cu, Hf, Li, Ni, Sc, Y, Pb, Th, Tl and U and around 5 % for Rb, Sr and the REE. The reproducibility was checked by analysis of international standards (JB3, JA2). Some trace elements were measured by both methods, the deviation of values is inside the reported errors. Results, obtained by XRF were generally preferred for elements with concentrations commonly larger than 20 ppm. The isotope ratios of Sr, Nd, and Pb were measured at the Finnigan MAT 252 in Göttingen. Sr and Nd isotope ratios were corrected for mass-fractionation to $^{86}\text{Sr}/^{88}\text{Sr}=0.1194$ and $^{144}\text{Nd}/^{146}\text{Nd}=0.7219$ and referenced to NBS987 (0.710245) and LaJolla (0.511847). Measured values of these standards over the period of the study were 0.710262 ± 24 and 0.511847 ± 20 . Lead isotopes were corrected to NBS981 (Todt et al., 1984). 13 measurements of this standard gave a mean of $^{206}\text{Pb}/^{204}\text{Pb}=16.90\pm 0.01$, $^{206}\text{Pb}/^{204}\text{Pb}=15.44\pm 0.02$ and $^{206}\text{Pb}/^{204}\text{Pb}=37,53\pm 0.05$. Blanks for Sr, Nd and Pb are <1ng, <0.03ng and <0.5ng accordingly, which have no influence on the results. From continuous measurement of standards and double measurements of samples, relative 2σ -errors less than 0.004 % for Sr and Nd, and less than 0.1 % for Pb were determined.

Regional geology and petrology

Bakening volcano main cone

The Bakening volcano (2277 m) is 5 km wide in diameter and rises around 1500 m over its basement. From W its shape is a relatively good preserved cone. The internal structure of the stratovolcano can be best studied from the SE side, where a gravitational collapse exposed deeper sections. This collapse produced a debris avalanche, which was dated at 8000-8500 years B.P. (^{14}C) (Melekestsev et al., 1998). The lower part exposes strongly altered Tertiary volcanic and volcanoclastic rocks of the basement. This alteration is probably connected with the injection of Bakening andesites into these rocks. Less altered Tertiary rocks can be found in the S and W of the volcano. A great number of Quaternary andesitic and dacitic intrusions and block lava flows are piled up on this basement to a high of around 1000 m. In the upper part of the volcano the remains of the former crater are preserved and documented by strongly altered crater sediments. Numerous dikes are eroded out at the slopes by erosion. With 150 m the highest of them is called Ditmar's Obelisk, to honor the first geologist, who studied Bakening volcano in 1854 (Ditmar, 1890).

Two suites of rocks at Bakening stratovolcano are distinguished: The older stage of Bakening activity is represented by dacitic extrusions at the S and SW flanks between 1300 and 1700 m. These rocks are light gray, but often oxidized to a reddish color. They contain around 15-20 % plagioclase, 3-5 % amphibole and 1 % magnetite in a fine-grained groundmass. Amphibole crystals are long prismatic and show often opacite rims. They also occur in cumulates additionally composed of plagioclase, magnetite and glass.

The second rock type is represented by pyroxene andesite flows, which cover the whole volcano and form the dikes. These relatively well-preserved dark rocks are amphibole-free and contain 25-30 % plagioclase, 5-10 % dark green ortho- and clinopyroxene, 1 % magnetite and sometimes relicts of yellow-green olivine in a glassy to fine-grained groundmass. Olivine grains are partly reacted to orthopyroxene and magnetite. Phenocrysts are small, generally about 1 mm, rarely up to 5 mm. At the E slope of Bakening red tuffs are observed, which belong to the pyroxene andesite suite. Bakening volcanics frequently contain xenoliths of sedimentary and volcanic rocks of the basement, xenoliths of older Bakening eruptions and cumulates.

Activity of Bakening stratovolcano presumably began in Late Pleistocene times. Some flows are clearly Holocene, the youngest eruptions at the SE slope are only 3500 years old (Melekestsev et al., 1998).

Novy Bakening and comparable andesitic to dacitic cones

Bakening stratovolcano is surrounded within 5 km by six small andesitic to dacitic cones (Fig. 4-1). Novy Bakening, situated in the NNE of the stratovolcano, is the largest, youngest and best preserved. It is composed of 8 dacitic flows, flowing in E and W directions from the 250 m high eruption center. The lava contains around 10 % plagioclase and less frequently pyroxene (up to 2 %) and amphibole (up to 4 %). The lower flows are slightly more amphibole enriched compared to the upper flows but do not contain pyroxene. Two similar small extrusions just to the N suggest, that the eruption started from a nearly N-S directed fissure and concentrated later on Novy Bakening. The largest 5 km long flow was erupted to the W into a glacier valley. The small extrusion at lake Vysokoe W of Bakening is similar in mineral composition to Novy Bakening rocks (7 % plagioclase, 3 % amphibole). Compared to it, the cones SW of Bakening at the Malye lakes contain more plagioclase (20 %) and similar low amounts of pyroxene (1-2 %) and amphibole (2-3 %) and therefore are more similar to the older extrusions at Bakening main cone. Their flows are overlain by pyroxene-andesite flows of Bakening.

Basaltic monogenetic centers

Basaltic monogenetic volcanic centers can be found W of Bakening, at Srednaya Avacha river and its right tributary Kostakan river, in the Kavyche valley, and around 30 km to the E in the Levaya Avacha valley (Fig. 4-1). The eruption age is deduced from morphology and tephrochronology to Late Pleistocene to Holocene. The ages of the youngest cones are 600-1200 ¹⁴C years B.P. (Dirksen and Melekestsev, 1998). The crystallization sequence is olivine → olivine+clinopyroxene → olivine+clinopyroxene+plagioclase → plagioclase. Olivine is up to 1 mm in size, contains Cr-spinell inclusions, and shows often skeletal growth. Clinopyroxene is absent or less frequent than olivine except for samples from the pass between Srednaya Avacha and Kavyche valley. Clinopyroxenes in these samples are

elongated and show hourglass structures. Such clinopyroxenes also occur in the groundmass of the other basalts.

Rhyodacitic monogenetic centers

We sampled rhyodacitic thuyas at the NW base of Bakening, at the Avachinskoe lake and in the Kavyche valley. Similar highly differentiated rocks also occur further to the N at the NW slope of the Ganalsky ridge. They are formed by chilled volcanic rocks and contain plagioclase and minor amounts of biotite and clinopyroxene in a fine-grained groundmass. The black obsidian from the thuya at Kavyche river is phenocryst-free.

Plateau basalts

In the N of Bakening, in the Srednaya Avacha and the Kavyche valleys remnants of plateau-forming basalts and basaltic andesites are exposed. These so-called “plateau basalts” were formed from Miocene to Lower Quaternary all over Kamchatka. Detailed studies about the frequency and duration of eruptions are absent. Some age data is given by Kepezhinskis et al. (1997), which distinguish between a tilted Older series (~14 Ma) and a subhorizontal Younger series (2.6-3.0 Ma). Our samples belong entirely to the Younger series, which is equivalent to the K-Na-alkali-olivine basalts, described by Volynets (1994). Glacially dissected Lower Pleistocene plateau basalts occur from 800 m to 1500 m above sea level and form the base of Novy Bakening and of Bakening volcano except in its S. At the W side of Levaya Avacha valley in the S of Bakening they are absent. Single lava flows are tenths of meter thick and extend over km. Our samples are derived from locations N and NNW of Bakening volcano (Fig. 4-1). The mineral mode is similar to the Quaternary basalts but phenocrysts are less frequent and smaller in size.

One flow NNW of Novy Bakening is rich in xenoliths (dunites, harzburgites, green and black pyroxenites). After Koloskov et al. (1997) these xenoliths are derived from the transition zone between the plagioclase and spinell stability fields in the lithospheric mantle below Bakening, which is a potential component in Bakening magmas. For some of these xenoliths Kepezhinskis and Defant (1996) assume enrichment by carbonate-rich melts.

Geochemistry

Major elements

The entire range of Quaternary rock types, occurring at Bakening volcano were sampled and analyzed for major elements by XRF (Tab. 4-1). All samples are fresh and have low LOI (< 1 %) and low $\text{Fe}_2\text{O}_3/\text{FeO}$ ratios (< 0.3-0.6). The plateau basalts have slightly higher $\text{Fe}_2\text{O}_3/\text{FeO}$ ratios between 0.4-0.8 probably from slight alteration of these older rocks. Dacites of Bakening extrusions are slightly more oxidized up to $\text{Fe}_2\text{O}_3/\text{FeO}$ ratios of 1.0. No correlation between LOI and degree of oxidization or major and trace element contents exists. All samples follow a calc-alkaline trend (Fig. 4-2), except some of the most mafic plateau basalts, which are slightly alkaline.

Pleistocene and Holocene monogenetic centers reach from high-Mg basalts with 49 % SiO_2 , 10 % MgO and 16 % Al_2O_3 to high-Al basaltic andesites with 56 % SiO_2 , 4 % MgO and 20 % Al_2O_3 (Fig. 4-3). The decrease in MgO is coupled with a decrease in FeO, CaO and TiO_2 and an increase in SiO_2 , Na_2O , Al_2O_3 and P_2O_5 (Fig. 4-3). No systematic variations are observed for MnO and K_2O . Two slightly alkaline basaltic samples (O35, BAK64) show strongly increased TiO_2 , Na_2O and P_2O_5 contents. There exist no obvious relationship between the geochemistry and sequence of eruptions of the monogenetic centers.

Plateau basalts, differ significantly from the younger basalts by higher concentrations in TiO_2 , K_2O , Na_2O , and P_2O_5 , and lower concentrations in Al_2O_3 and CaO (at given MgO).

The Bakening stratovolcano is composed of andesites and dacites with SiO_2 of 60 to 66 %. Mineralogically and geochemically they are similar to the nearby small isolated mostly dacitic centers. A compositionally gap exists between the basaltic and dacitic suite from 56 to 60 % SiO_2 . Concentrations of FeO, CaO, MnO, MgO and TiO_2 are decreased, concentrations of Na_2O and K_2O increased compared to the basaltic rocks (Fig. 4-3). The youngest amphibole-free flows of the Bakening stratovolcano are the most mafic rocks of the dacitic suite and form different trends compared to the other andesites and dacites.

Trace elements and isotopes

Variations for certain trace elements versus MgO are shown in Fig. 4-4. Compatible trace elements like Sc, Co, V, Cr, and Ni have high abundances in the basaltic rocks and are strongly negative correlated with MgO or the magnesian number ($\text{Mg\#} = \text{Mg}/(\text{Mg} + \text{Fe}) \text{ mol\%}$).

The most mafic sample BAK24 contains 500 ppm Cr and 170 ppm Ni at an Mg# of 65. It can be regarded as close to a primary magma composition. In comparison, dacitic rocks are more depleted in compatible elements. Incompatible trace elements such as Ba, Pb, Zr, Nb and the La/Yb ratio increase slightly with decreasing MgO in the basaltic and stronger in the dacitic rocks. Sr contents increase in the basaltic but remain almost constant in the dacitic rocks. This behavior is comparable with Al_2O_3 .

Again the two basaltic samples O35 and BAK64 are enriched in some trace elements (Sr, Zr, Nb and La/Y) and again they show a similarity to the plateau basalts, which are also enriched in all HFSE, Sr and the LREE relative to the normal Bakening basalts.

From one cumulate, enclosed in an amphibole-bearing dacite of the Bakening volcano, concentrates of amphibole and plagioclase were separated and measured by ICPMS for trace elements (Tab. 4-2). This cumulate consists of ~20 % amphibole, ~40 % plagioclase and ~40 % interstitial glass. The amphibole of the cumulate is enriched in the middle to heavy REE compared to the presumed dacitic parent (Tab. 4-4). The highest enrichment (3x) is found for Dy. REE concentrations in plagioclase are negligibly low. These measurements are in agreement with the reported mineral/melt distribution coefficients in andesitic and dacitic systems (Dunn and Sen, 1994; Fujimaki et al., 1984; LaTourrette et al., 1995; Sisson, 1994).

The overall trace element pattern for Late Quaternary rocks is generally similar and typical for island arc rocks (Fig. 4-5). Fluid mobile trace elements are strongly enriched and HFS elements relatively depleted. The enrichment decrease with decreasing element incompatibility. Ba, Rb, U, Th and K have more than 10 times higher concentrations compared to NMORB. Dacitic rocks show an even stronger gradient from the highest incompatible to less incompatible elements than the basaltic rocks. Nb and Ta have low concentrations like in the basaltic rocks similar to NMORB. HREE are more strongly depleted. The plateau basalts mostly overlap with the younger basalts, except in their less pronounced HFSE depletion. The REE-pattern of all samples of the Bakening area crosses each other (Fig. 4-6) and the HREE in the dacitic are still lower than in the basaltic rocks.

The Sr, Nd and Pb isotopic composition is very similar for all rocks of the Bakening area and only slightly more radiogenic than MORB. Its variation is inside the field for other Quaternary volcanics of Kamchatka (Churikova et al., 2000).

Some of the differences in major and trace elements are clearly caused by mineral fractionation. Therefore in next chapter we first want to examine the fractionation history of the rocks of the Bakening area.

Discussion

Fractional crystallization

Basaltic suite

Major element variations are mainly controlled by the fractionation of olivine and clinopyroxene, which strongly deplete the magma in MgO, CaO, FeO and compatible trace elements (Cr, Co, Ni, Sc, V). Straight trends indicate, that the ratio between the fractionating minerals was more or less the same, regardless the different observed abundance of phenocrysts in the samples. Significant plagioclase and amphibole fractionation can be excluded for the majority of the samples from MgO versus Al₂O₃ and Sr (Figs. 4-3 and 4-4). Only at MgO < 5 % a limited plagioclase fractionation occurred, which is evident from decreasing Al₂O₃. The slightly alkaline basalts O35 and BAK64 that lack plagioclase phenocrysts fall off this fractionation trend. They probably formed from a distinct parental magma, which was higher enriched in Ti, Na and P, similarly to that of the plateau basalts. The linear trend of decreasing TiO₂ at decreasing MgO in the basaltic samples is problematically, because all fractionating phases, except magnetite, have $D_{\text{mineral/melt}} < 1$ for Ti. There is no indication for amphibole crystallization in the basaltic magmas. The observed Ti depletion in the basaltic rocks can be attained by only ~1 % magnetite fractionation. However, (titano?)magnetite as phenocryst was detected in only 3 of 31 samples. In two of these cases additional samples from the same lava flow did not contain magnetite, despite similar Ti-concentrations. This indicates that magnetite crystallization in the basaltic magmas occurred just before or in the cause of eruption and had no influence on Ti-fractionation. However, we cannot exclude an early high-pressure magnetite fractionation as inclusions in mafic minerals. More likely it seems, that clinopyroxene is more Ti-rich than predicted by most of the experimentally determined distribution coefficients in basaltic systems. A strong evidence for this hypothesis are the hour-clock structures of the clinopyroxenes, which indicates a high Ti-content.

Dacitic suite

Mineralogy and element variations indicate that the major element variations of the dacitic suite are caused by fractionation of amphibole, plagioclase, ortho- and clinopyroxene, magnetite and apatite from an evolved member of the basaltic suite (Fig. 4-3). This assemblage has a relatively low MgO and high SiO₂ content compared to the fractionating

minerals in the basalts, which cause in different element trends versus MgO and SiO₂ for the two suites. The gap in SiO₂ between the basaltic and dacitic rocks can be explained by extensive plagioclase and amphibole (both minerals are enriched in SiO₂ and depleted in MgO compared to the melt) fractionation in the magma chamber before eruption. This is proved by the fact, that no gap exists for MgO, which is not much affected by plagioclase and amphibole fractionation. Plagioclase fractionation is also evident from the decrease in Al₂O₃ and Sr.

The youngest cpx-opx-andesite flows are the most mafic rocks of the Bakening stratovolcano in respect of the MgO content (Fig. 4-3). Their trends are distinct from the trend of the other andesites and dacites. Major and trace elements suggest, that their parental magma was formed by mixing of a basaltic magma into the dacitic magma chamber of Bakening volcano (Figs. 4-3 and 4-4). Mixing between a basaltic (BAK4) and dacitic (BAK35) end member was modeled in Figs. 4-3 and 4-4. These two magmas must have been homogenized and fractionated before eruption, because the analyzed samples do not fall on a mixing line, but on a fractionation trend originating from a point on the mixing line with a composition of about 70 % dacitic and 30 % basaltic component. Macroscopically and microscopically no mixing textures could be found. Occasionally plagioclase occurs with sieve structures and olivines rimmed with fine-grained aggregates of orthopyroxene indicating disequilibrium conditions in the microscopic scale.

Ti even stronger decrease in the dacitic compared to the basaltic samples. However magnetite is abundant in all dacitic rocks (1 %), and can easily explain this observation. Amphibole fractionation can also produce a significant Ti-depletion. Up to 0.5 % apatite fractionation must have occurred to produce the decrease of phosphorus in the dacitic rocks (Fig. 4-3).

From the enrichment of highly incompatible elements (Ba, Rb, U, Th), the degree of fractionation can be estimated. If the most primitive basalt BAK24 is chosen as parent, between 50 and 80 % fractionation must have occurred to produce the dacitic rocks.

REE-pattern

Major element variations suggest, that the basaltic and dacitic suites are connected by fractionation. Additionally for the cpx-opx-andesites of Bakening mixing between basaltic and dacitic magmas can be supposed. Increasing REE contents and LREE/HREE ratios are generally observed trends from basaltic to dacitic rocks, which is caused mainly by fractionation of olivine, pyroxene and plagioclase. The decrease in MREE and HREE contents

in the dacitic compared to the basaltic rocks needs a different explanation (Fig. 4-7). Clinopyroxene and amphibole reach $D_{\text{mineral/melt}} > 1$ for the MREE and HREE in andesites and dacites. Apatite can also have a significant influence on the REE pattern despite its small amount in the fractionation, because it has very high $D_{\text{mineral/melt}}$ for all REE. It depends from the amounts of fractionating clinopyroxene, amphibole and apatite compared to the amount of plagioclase and orthopyroxene, how much the LREE are enriched relatively to HREE and if an absolute depletion in MREE and HREE can be produced. Such depletion should be more likely in SiO_2 rich samples, corresponding to our observations.

A simple last squares calculation of the relationship between a primitive member of the basaltic suite (BAK24) and a member of the dacitic suite (BAK03) yields a good approximation of the REE for a fractionation of 20 % amphibole, 12 % plagioclase, 7 % clinopyroxene, and 0.6 % apatite (Tab. 4-4, Fig. 4-7). $D_{\text{mineral/melt}}$ values for calc-alkaline andesites of Fujimaki (1986); Fujimaki et al. (1984) were used for this calculation. Clinopyroxene in this data set has relatively low D-values compared to amphibole. Applying partition coefficients from other sources would result in different amounts of fractionating minerals and probably lower amounts of amphibole. However, additional evidence for an amphibole-dominated fractionation in the evolved rocks comes from amphibole-rich cumulates, occasionally occurring in the older Bakening dacites. The REE-contents of amphibole from such cumulate (Tab. 4-3) emphasize the role of amphibole for the HREE-depletion in the dacitic rocks.

Different REE pattern were reported from various arcs, whereby back-arc basalts show higher La/Yb ratios and sometimes a pronounced HREE depletion compared to volcanoes at the front (see compilation in Tatsumi and Eggins (1995)). Such increase in La/Yb across the arc was also shown for mafic volcanics from Kamchatka (Churikova et al., 2000). This pattern was explained by residual phases with high D-values for the HREE in the melting region (Tatsumi and Eggins, 1995). Therefore alternatively we want consider source variations as probable reason for the differences of the REE pattern in our two suites.

Also if we deny that fractionating phases have influenced the shape of the REE pattern, we have to consider their amount, to correct the pattern to a primary melt composition. This correction shifts the pattern to lower concentrations without changing of the shape. Such behavior was shown for the Ksudach volcano (Volynets, 1994) where REE contents increase from basaltic to dacitic rocks by a factor of 3 without a significant change in the La/Yb ratio. Applying these results on our dacitic series, we get a pattern, which is extremely depleted in

HREE compared to the basaltic suite (3 times) and NMORB (5 times) and reaches almost the mantle value in Yb. It is not possible to model such composition with the established models of mantle melting.

We therefore conclude, that the observed REE pattern of the dacitic rocks can only be produced by fractional crystallization from a pattern like in the basalts. The reason for the relatively low HREE contents in the basalts compared to MORB shall be discussed in the following chapter.

Source composition

Modeling of the observed HREE contents of basaltic rocks by melting an NMORB-source gives high melting rates of about 30 %. This is higher than the 10-25 % melting inferred by Plank and Langmuir (1993) for typical arc volcanism. If the N-MORB source is depleted by 10 % melt extraction we get more reasonable melting degrees of 15-20 %. Residual phases have also some influence on the REE pattern. At low melting degrees garnet, clinopyroxene or amphibole in the residuum can produce relatively HREE depleted melts. Amphibole will not produce much different pattern compared to clinopyroxene, because of their nearly similar D values (Hart and Dunn, 1993; LaTourrette et al., 1995). At 15 % melting degree of an ultra-depleted mantle, both phases are completely consumed in the melt and will have no influence on the REE-pattern. Garnet as residual phase can be stable at low melting degrees. However its influence must be limited, because it produces a steep range in the HREE, which is not observed in the samples.

Mantle depletion is expressed in the Nb/Zr ratio as well because Nb is stronger depleted compared to Zr after mantle melting. Both elements are not much influenced by fluid enrichment (Ayers and Eggler, 1995; Brenan et al., 1995b). The Nb/Zr ratio is also not influenced by fractional crystallization (Fig. 4-8 and Tab. 4-3). Nb/Zr against Nb shows a positive trend in the basaltic and dacitic rocks. This trend is partly produced by the relatively large analytical error for Nb. However, all plateau basalt and some Late Quaternary basaltic rocks are clearly displaced to higher Zr and Nb concentrations and higher Nb/Zr ratios. The Zr enrichment is even more pronounced in Zr versus Ba/Zr, where at a nearly constant Ba concentration Zr is strongly enriched. This higher HFSE concentrations can result from a more primitive mantle source or were caused by melt enrichment. The Nb/Zr ratios of the

Baking rocks reach from enriched to depleted compared to NMORB. We believe, that this trend represent mixing between depleted and enriched mantle sources.

Fluid enrichment in the source

Ratios of incompatible elements can be used to get information about the magma source composition. The dacitic suite and the rhyodacites however, have to be evaluated with caution because even fractionation of minor phases like biotite, apatite and zircon, occurring in such evolved rocks in low abundances can strongly influence the noted elements. Also substantial amphibole fractionation can influence incompatible element ratios.

With these precautions in mind, ratios of fluid and melt mobile (K, Rb, Ba, U, Th) over fluid immobile but melt mobile (Zr, Hf, Nb, Ta) trace elements are a powerful tool to study the source enrichment by slab-derived fluids. For example the Ba/Zr ratio in the basaltic suite is variable from 1.8 to 4.9 (Fig. 4-8). Dacitic samples have 3.8-4.6 in Ba/Zr inside the basaltic range rocks. Plateau basalts are lowest in Ba/Zr from 1.3 to 2.6, caused by the high Zr concentrations in more mafic samples.

The Ba/Zr ratio in basaltic samples is independent of their degree of differentiation (i.e. MgO content). Therefore fractionation did not affect this ratio. It is also unlikely, that variable degrees of partial melting have affected Ba/Zr because of low partition coefficients in mantle minerals. We conclude, that variable Ba/Zr ratios reflect slightly distinct mantle sources, probably affected by variable degrees of slab-fluid enrichment.

Miller et al. (1994) used the Ce/Pb ratio as tracer for the amount of slab fluids involved in the source. Such fluids are highly enriched in Pb compared to the REE (Brenan et al., 1995a) and therefore variations in fluid enrichment, e.g. variable Ba/Zr ratios should correlated in Ce/Pb. The Ce/Pb ratios in the basaltic suite are variable from 11.2 to 6.6. In comparison, the Ce/Pb ratios in dacitic samples reach from 4.5 to 5.8, i.e. they are lower and less variable than in the basaltic rocks. The nearly horizontal trend for the dacitic rocks in Ce/Pb versus MgO suggest, that the Ce/Pb ratio is not changed by fractionation up to dacitic compositions and that the low ratios are a characteristic of the source. A variable fluid induced Pb enrichment of the source is proven by the negative trend between Ce/Pb and Pb in the basaltic rocks. The Ce/Pb ratios are correlated with the Ba/Zr ratios.

Isotopic constraints

Sr- Pb- and Nd-isotope ratios are close to the MORB field (Fig. 4-9). In Sr-Nd space, the data are slightly shifted to a more radiogenic Sr isotopic composition, compared to MORB. This pattern is typical for most Kamchatka rocks and was interpreted as a mixture of slab fluid and the depleted mantle wedge (Churikova et al., 2000). The amount of sediment in the source for Kamchatka arc rocks was estimated on the basis of Pb-, Sr-, Nd- and Be-isotopes to be less than 1 % (Bailey, 1996; Kersting and Arculus, 1995; Turner et al., 1995).

The rocks of the Bakening area are relatively low and overlap in $^{87}\text{Sr}/^{86}\text{Sr}$ compared with other rocks of Kamchatka, indicating a lower amount of fluid or sediment. A tendency in the dacitic suite to more radiogenic values exists. However there is no correlation with SiO_2 or Mg# and the most evolved rhyodacite BAK19 has an isotopic composition identical within error to the basaltic rocks. This arguments against a significant role of assimilation of old crust. However, because the Kamchatka crust is young, with relatively unradiogenic Sr we cannot completely exclude assimilation. The Sr-isotope ratio of one analyzed plateau basalt is the most radiogenic in the Bakening area, but still within the field for typical Late Quaternary rocks.

Source of the plateau basalts

The number of studied plateau basalts analyzed here is limited and only preliminary interpretations can be given. All plateau basalts have LILE concentrations comparable to, or even slightly higher than, Late Quaternary Bakening rocks. Most remarkable are the strong enrichment in Ti, Na, K, P, Sr, HFSE, LREE and depletion in Ca and Al. This results in low LILE/HFSE and high LREE/HREE ratios. High Ce/Pb ratios between 11 and 20 and low Ba/Zr ratios are caused by high Zr and Ce concentrations (Fig. 4-8). The Zr content decrease with an increase in SiO_2 or decrease in MgO, respectively (Fig. 4-4) and some elements (K: 1.1-1.9 %; Sr: 540-850 ppm) are strongly scattered, excluding, that these rocks are derived from a similar source. The HREE are similar depleted like in the Late Quaternary basalts.

Kepezhinskas and Defant (1996) suggested from the study of xenoliths from plateau basalts N of Bakening, that parts of the mantle were metasomatized by carbonate-rich melts. These melts were be assumed slab derived. Clinopyroxenes from such metasomatized xenoliths were described to be enriched in Cr, Mg, Al, Ti, Na, Sr, Nb, Zr and REE compared to unmetasomatized xenoliths. The metasomatizing component is thus characterized by a high

La/Yb, Zr/Hf, Sr/Sm, Nb/La and low Ti/Eu and Y/Er. However, a marine sedimentary component can be excluded, based on the low $^{87}\text{Sr}/^{86}\text{Sr}$, determined in one sample of plateau basalts. Moreover Sr-, Nd- and O-isotope measurements on pyroxene separates from xenoliths, derived from the plateau basalts have yield values similar to the Late Quaternary samples from Bakening (unpublished data of M.Puzankov). No increase or decrease is detectable in the plateau basalts for Zr/Hf, Sr/Sm, Nb/La and low Ti/Eu and Y/Er, respectively compared to the Late Quaternary basalts and to other basalts of Kamchatka.

We propose, that fluid induced melting of a mixture of enriched and depleted mantle sources produced the plateau basalts. Enriched mantle has low HREE concentrations similar to depleted mantle but contains significantly higher concentrations of incompatible elements (LILE, HFSE). The LILE enrichment of the enriched mantle (EM) is small compared to the contribution from the slab fluid and therefore the EM pattern of the LILE is completely overprinted. In difference HFSE elements are not carried by the fluid and their enrichment therefore depends on the relative amount of the EM component in the source. A similar two component mixing model was developed by Volynets et al. (1997) for Miocene within-plate type basalts from the Valaginsky range/Eastern Kamchatka. They argue from a large Sr-Nd-O-isotope variation in these rocks for mixing of an OIB-type mantle plume (EM1) into the arc magma source. However, our preliminary results could not show such large isotopic variations so far. Further isotopic studies and exact age determinations on the Bakening plateau basalts are necessary to prove and develop the model of plateau basalt genesis in the island arc environment.

Two of the Late Quaternary basaltic rocks (O35, BAK64) show a tendency to a plateau basalt pattern and suppose that source inhomogenities have survived until Recent.

Conclusions

Major elements argue for a close relationship between the bimodal Late Quaternary basaltic and dacitic suites in the Bakening area. The fractionation in basaltic rocks starts with olivine and clinopyroxene, plagioclase is additional abundant in more evolved rocks. Fractionation in dacitic rocks is determined by amphibole, plagioclase, clinopyroxene, orthopyroxene and additional low amounts of magnetite and apatite.

Basaltic samples show a range of variably enriched sources, probably caused by different degrees of fluid enrichment and mantle depletion. Dacitic rocks have at the first view a similar trace element pattern like basaltic rocks (Fig. 4-5). Slight differences in LILE and the remarkable HREE depletion can be produced by amphibole fractionation. However regarding Ba/Zr and Ce/Pb the dacitic suite must be derived from a source, which was similar or even more enriched in fluid mobile elements like the most enriched source of the basaltic suite. Plateau basalts were probably derived from a mixture of depleted and enriched sources, which were overprinted by the slab fluid.

Tab. 4-1 Major [wt.%] and trace element [ppm] data of Quaternary volcanics in the Bakening area

	Basalts and basaltic andesites from monogenetic centers																Mount Peschanaja				
	Levaya Avacha valley					Kostakan						Mount Peschanaja									
	BAK04	BAK24	BAK61	BAK62	BAK49	BAK43	BAK44	BAK45	BAK47	BAK64	BAK42	BAK31	BAK37	BAK30	BAK34	BAK32	BAK33	BAK41	O-40	O-26	O-35
SiO ₂	48.75	49.68	50.40	50.40	51.41	51.70	52.08	52.46	52.63	53.30	53.55	50.26	50.37	50.53	51.16	51.23	51.32	51.50	49.77	50.41	51.49
TiO ₂	1.13	1.03	1.06	1.07	0.90	0.91	1.05	0.89	0.89	1.36	0.98	1.09	1.09	1.08	1.04	1.02	1.03	1.02	1.20	1.10	1.29
Al ₂ O ₃	17.26	16.22	16.70	16.65	17.80	18.43	17.07	19.22	19.33	16.81	16.72	16.10	16.30	16.29	16.88	16.70	16.76	16.99	16.84	16.28	16.70
Fe ₂ O ₃	2.68	2.46	3.00	2.83	2.59	2.21	2.72	2.77	3.06	3.39	2.48	2.24	2.26	2.58	2.08	1.93	2.35	1.91	3.10	2.53	3.00
FeO	7.09	6.91	6.25	6.45	6.19	6.50	5.92	5.95	5.80	5.63	5.35	6.89	6.86	6.56	6.70	6.86	6.56	6.74	6.12	6.42	5.52
MnO	0.17	0.17	0.16	0.17	0.17	0.16	0.15	0.17	0.17	0.15	0.14	0.17	0.17	0.17	0.17	0.17	0.17	0.17	0.16	0.15	0.15
MgO	8.09	9.83	8.51	8.61	6.63	5.74	7.47	4.59	4.65	6.02	7.28	9.15	8.84	9.05	7.80	8.09	8.32	7.56	8.61	9.40	6.72
CaO	10.47	9.67	9.07	9.09	8.82	8.77	8.51	8.36	8.45	7.80	7.92	9.32	9.27	9.22	8.94	9.01	9.06	8.91	9.60	9.06	9.52
Na ₂ O	2.83	2.87	3.16	3.20	3.27	3.32	3.48	3.75	3.69	3.96	3.70	3.21	3.15	3.16	3.18	3.16	3.14	3.21	3.24	3.22	3.56
K ₂ O	0.70	0.70	0.89	0.91	0.67	0.90	0.91	0.87	0.86	1.07	1.04	0.95	0.95	0.94	0.91	0.91	0.92	0.92	0.88	0.90	1.22
P ₂ O ₅	0.17	0.21	0.23	0.23	0.23	0.25	0.26	0.31	0.31	0.42	0.29	0.26	0.26	0.26	0.23	0.23	0.23	0.23	0.24	0.28	0.41
LOI	0.25	0.60	0.56	0.46	0.54	0.49	0.16	0.47	0.17	0.30	0.36	0.27	0.20	0.32	0.47	0.49	0.43	0.41	0.31	0.23	0.53
Total	99.58	100.34	100.00	100.06	99.21	99.38	99.77	99.81	100.00	100.22	99.81	99.89	99.71	100.15	99.55	99.81	100.27	99.57	100.04	99.96	100.09
Li	8.2	6.0			7.5	8.2	6.9	7.8	6.9		5.7	8.5	6.1	8.0	8.1		7.5	7.5	6.8	7.2	8.1
Be	0.74	0.60			0.74	0.73	0.90	0.70	0.72		0.99	0.80	0.76	0.80	0.78		0.77	0.74	0.70	0.69	0.82
Sc	38	34	30	26	24	25	23	19	19	20	25	30	30	30	29	29	29	26	31	30	29
V	304	261	255	249	207	217	223	181	186	220	205	253	254	249	237	242	240	238	285	250	275
Cr	233	494	329	337	179	91	285	28	26	217	292	394	360	377	272	301	315	259	283	343	165
Co	38	46	39	42	31	33	36	26	29	34	34	44	41	43	38	41	43	38	44	43	35
Ni	84	169	141	170	69	46	126	17	25	75	122	155	152	155	117	125	134	111	127	167	62
Cu	63	63			48	43	52	41	27		25	68	64	63	58		59	52	52	40	80
Zn	69	77	81	80	70	75	74	84	82	100	80	76	76	76	74	73	74	73	71	71	75
Ga	16	17	20	16	14	16	17	18	19	20	17	17	17	17	17	17	17	17	17	17	17
Rb	27	15	14	18	13	18	18	16	15	15	20	22	25	19	20	17	19	18	12	17	21
Sr	429	423	496	494	526	536	525	628	627	708	563	505	512	497	471	468	463	475	518	547	706
Y	10	21	16	20	21	21	22	23	20	22	18	21	20	22	24	23	21	22	23	20	32
Zr	64	82	88	86	94	84	102	90	91	125	107	91	91	90	92	90	91	92	92	92	115
Nb	2.8	2.8			2.7	2.7	3.6	2.8	2.7		3.6	4.3	3.4	3.1	3.6		3.6	3.2	3.5	3.5	5.1
Cs	0.38	0.49			0.43	0.62	0.30	0.54	0.41		0.54	0.76	0.71	0.70	0.58		0.64	0.60	0.57	0.29	0.62
Ba	223	241			275	412	358	394	401	345	375	400	382	379	304	312	298	312	326	340	440
La	7.1	7.6	313	318	7.9	9.0	10.2	9.4	9.4		11.6	10.7	10.5	10.0	9.4	313	9.6	9.4	9.1	10.1	14.7
Ce	18.2	19.4			20.1	21.9	24.6	23.3	23.3		28.3	24.7	24.7	23.4	22.7	23.0	23.0	22.6	21.9	23.8	36.7
Pr	2.9	3.0			3.2	3.3	3.7	3.6	3.6		4.3	3.6	3.6	3.5	3.4		3.4	3.4	3.3	3.6	5.7
Nd	13.7	13.8			14.8	15.5	17.3	16.6	16.7		19.3	16.7	16.6	16.2	15.7		15.9	15.6	15.8	16.6	25.5
Sm	3.6	3.7			3.8	4.0	4.3	4.3	4.2		4.6	4.3	4.3	4.1	4.0		4.1	4.0	4.1	4.1	5.7
Eu	1.13	1.15			1.18	1.20	1.32	1.29	1.32		1.36	1.29	1.28	1.25	1.24		1.28	1.22	1.30	1.28	1.64
Gd	3.2	3.4			3.2	3.6	3.9	3.7	3.6		3.9	3.8	3.9	3.8	3.7		3.8	3.7	3.8	3.7	4.4
Tb	0.53	0.54			0.53	0.58	0.62	0.58	0.58		0.60	0.61	0.62	0.61	0.61		0.62	0.61	0.61	0.59	0.64
Dy	3.1	3.3			3.1	3.4	3.6	3.4	3.4		3.6	3.6	3.6	3.6	3.6		3.6	3.6	3.6	3.4	3.6
Ho	0.64	0.67			0.62	0.69	0.70	0.68	0.68		0.63	0.70	0.72	0.71	0.72		0.74	0.73	0.72	0.66	0.68
Er	1.81	1.88			1.82	2.04	1.93	2.01	2.03		1.83	1.99	2.07	2.01	2.08		2.10	2.12	2.10	1.91	1.88
Tm	0.27	0.27			0.27	0.31	0.29	0.30	0.31		0.26	0.28	0.29	0.29	0.31		0.31	0.31	0.30	0.28	0.26
Yb	1.80	1.81			1.76	1.92	1.81	1.96	1.95		1.72	1.85	1.88	1.89	1.96		2.03	1.98	1.89	1.79	1.69
Lu	0.27	0.26			0.26	0.30	0.26	0.31	0.31		0.25	0.28	0.28	0.28	0.30		0.30	0.29	0.29	0.26	0.25
Hf	1.85	2.08			2.09	2.21	2.60	2.35	2.33		2.77	2.37	2.44	2.35	2.35		2.42	2.33	2.33	2.38	2.84
Ta	0.18	0.33			0.18	0.22	0.21	0.18	0.20		0.18	0.27	0.18	0.15	0.20		0.23	0.20	0.23	0.22	0.29
Ti	0.05	0.04			0.06	0.01	0.05	0.04	0.05		0.05	0.06	0.05	0.07	0.09		0.06	0.08	0.03	0.03	0.09
Pb	2.1	2.3			2.5	2.9	2.9	3.3	2.9		2.7	3.5	3.8	3.5	2.9		3.2	2.9	2.8	2.8	3.7
Th	0.67	0.89			0.75	1.45	1.41	1.20	1.19		1.34	1.60	1.75	1.49	1.46		1.76	1.53	1.26	1.24	1.50
U	0.33	0.42			0.35	0.58	0.61	0.52	0.54		0.62	0.66	0.67	0.64	0.56		0.60	0.54	0.55	0.55	0.61

Tab. 4-1 Major [wt.%] and trace element [ppm] data of Quaternary volcanics in the Bakening area

	Basalts and basaltic andesites from monogenetic centers															Plateau basalts									
	Kavycha valley										Levaya Avacha valley					Bak01									
	BAK21A	BAK15	BAK14	BAK17	BAK18	BAK20A	BAK20B	BAK16	BAK38	BAK21B	23/7	23/8	BAK01	23	23/1	121	120	7760	BAK06						
SiO ₂	50.07	50.13	50.32	51.23	53.50	53.51	53.61	54.41	54.53	55.08	48.70	49.10	49.30	49.70	49.80	50.70	51.00	51.90	53.23						
TiO ₂	0.97	0.96	0.99	1.15	0.79	0.94	0.93	0.94	0.86	0.82	1.62	1.56	1.59	1.16	1.15	1.70	1.61	1.76	1.41						
Al ₂ O ₃	16.85	16.80	16.41	16.30	19.44	18.88	18.94	17.41	19.12	18.30	16.10	16.20	16.43	15.76	15.76	15.87	16.05	16.13	15.86						
Fe ₂ O ₃	3.34	2.60	2.18	2.01	2.34	3.11	2.38	2.41	3.26	1.94	11.18	10.80	3.50	2.81	4.30	2.94	2.94	4.00	3.39						
FeO	6.10	6.73	7.02	6.52	6.13	5.21	5.92	5.58	5.08	5.92	0.19	0.19	0.19	0.19	0.16	0.15	0.15	0.15	0.14						
MnO	0.19	0.19	0.18	0.16	0.17	0.15	0.15	0.16	0.17	0.15	0.19	0.19	0.19	0.16	0.16	0.15	0.15	0.15	0.14						
MgO	8.24	8.33	8.92	8.29	3.93	4.57	4.50	5.32	3.85	3.75	7.80	7.84	7.54	9.30	9.17	8.84	9.03	6.47	5.77						
CaO	9.47	9.51	9.74	8.90	8.27	8.25	8.29	8.48	7.66	7.20	8.40	8.19	8.34	9.33	9.33	8.18	8.15	8.52	7.74						
Na ₂ O	2.91	3.00	3.00	3.38	3.75	3.68	3.68	3.46	3.87	3.80	3.72	3.82	3.82	3.05	3.72	3.66	3.72	3.66	3.66						
K ₂ O	0.75	0.77	0.68	1.01	0.81	0.90	0.90	1.13	0.96	1.20	1.68	1.73	1.88	1.35	1.36	1.07	1.09	1.12	1.08						
P ₂ O ₅	0.26	0.26	0.23	0.23	0.29	0.23	0.24	0.21	0.25	0.24	0.46	0.43	0.44	0.39	0.39	0.44	0.45	0.51	0.34						
LOI	0.21	0.51	0.49	0.60	0.45	0.75	0.77	0.66	0.71	0.44	99.84	99.85	100.04	99.95	100.10	100.54	100.25	0.32	0.54						
Total	99.36	99.78	100.15	99.83	99.86	100.18	100.29	100.14	100.30	98.84	99.84	99.85	100.04	99.95	100.10	100.54	100.47	100.35	98.61						
Li		7.1	6.2	7.4	8.1	6.1	6.1	9.6	8.9	8.9				6.4	6.0			5.7	8.8						
Be		0.82	0.71	0.86	0.81	0.76	0.76	0.76	0.75	0.75				0.98	1.13			3.41	0.88						
Sc	29	32	33	29	17	20	20	27	16	21	26	25	26	28	30	21	22	26	24						
V	230	235	242	236	158	201	209	235	181	171	212	210	216	243	243	167	156	269	214						
Cr	311	317	411	349	15	29	30	104	15	15	255	260	220	545	539	340	362	237	191						
Co	38	40	41	38	27	28	29	32	24	25	38	40	37	43	47	40	40	32	30						
Ni	117	121	126	130	11	17	18	32	6	0	133	131	129	230	227	249	257	80	38						
Cu		55	60	52	37	56	56	38	38	34				76	34			19	35						
Zn	78	80	77	75	88	78	79	77	77	70	70	69	83	75	76	86	80	106	93						
Ga	18	17	17	16	19	19	18	18	19	18	16	18	18	17	15	16	18	19	16						
Rb	11	21	17	21	17	15	15	22	15	17	22	24	23	26	28	13	16	13	0						
Sr	514	531	453	529	628	605	609	481	596	567	626	629	614	558	554	538	550	846	591						
Y	3	24	24	23	22	19	21	21	18	23	30	30	28	21	20	32	30	20	8						
Zr	101	96	96	108	93	92	90	85	86	99	155	162	160	117	119	208	214	140	128						
Nb		2.3	3.0	4.7	2.8	2.4	2.4	3.1	3.1	3.1				7.5	7.5			7.3	6.7						
Cs		0.59	0.45	0.64	0.45	0.47	0.47	0.67	0.49	0.49	238	259	287	0.60	0.43			0.30	0.44						
Ba	184	194	185	346	328	335	336	358	336	375				329	314		281	361	288						
La		8.9	8.1	11.0	9.6	9.8	9.8	9.9	9.5					12.5	12.7			13.9	12.6						
Ce		23.2	21.5	26.7	23.7	23.5	23.5	23.3	22.6					30.8	31.1			35.7	30.5						
Pr		3.7	3.4	4.0	3.6	3.5	3.5	3.4	3.4					4.6	4.7			5.5	4.7						
Nd		17.4	15.7	18.6	16.4	16.1	16.1	15.3	15.5					20.9	21.2			25.5	21.2						
Sm		4.5	4.1	4.7	4.1	4.0	4.0	3.9	3.9					5.1	5.2			6.2	5.3						
Eu		1.32	1.28	1.39	1.26	1.22	1.22	1.16	1.21					1.49	1.48			1.77	1.52						
Gd		4.0	3.8	4.1	3.4	3.4	3.4	3.4	3.3					4.2	4.3			4.9	4.5						
Tb		0.66	0.64	0.65	0.56	0.54	0.54	0.56	0.54					0.64	0.64			0.73	0.71						
Dy		4.0	4.0	3.8	3.2	3.2	3.2	3.3	3.1					3.6	3.6			4.0	4.0						
Ho		0.81	0.83	0.75	0.63	0.64	0.64	0.68	0.63					0.67	0.68			0.73	0.77						
Er		2.34	2.38	2.17	1.91	1.87	1.87	1.89	1.91					1.84	1.88			1.95	2.15						
Tm		0.35	0.36	0.32	0.29	0.28	0.28	0.28	0.28					0.26	0.26			0.27	0.31						
Yb		2.23	2.33	2.04	1.82	1.76	1.76	1.85	1.85					1.66	1.69			1.72	1.92						
Lu		0.34	0.34	0.31	0.28	0.27	0.27	0.27	0.28					0.26	0.25			0.25	0.29						
Hf		2.48	2.41	2.73	2.35	2.35	2.35	2.27	2.25					2.64	2.62			3.16	3.19						
Ta		0.11	0.45	0.29	0.19	0.17	0.17	0.22	0.20					0.48	0.49			0.61	0.48						
Tl		0.04	0.05	0.08	0.07	0.09	0.09	0.06	0.08					0.04	0.01			0.03	0.05						
Pb		2.1	2.1	2.8	3.1	3.1	3.1	3.5	3.5					1.8	1.5			2.9	2.7						
Th		0.95	0.81	1.42	1.08	1.36	1.36	1.77	1.16					1.31	1.32			1.11	1.24						
U		0.52	0.44	0.60	0.48	0.55	0.55	0.70	0.53					0.68	0.69			0.48	0.46						

Tab. 4-1 Major [wt.%] and trace element [ppm] data of Quaternary volcanics in the Bakening area

	Bakening andesites/dacites				2px-andesites				Andesitic/dacitic centers around Bakening				Thuya rhodacities									
	amph-andesites		BAK12		BAK22	BAK39	BAK23	BAK40	O-71	BAK11	BAK13	SW Bakening		Novy Bakening		Levaya Avacha v.		Kavyche v.				
	BAK10	BAK11	BAK22	BAK39	BAK23	BAK40	BAK23	BAK40	O-71	BAK11	BAK13	BAK35	BAK36	BAK25	BAK03	BAK05	BAK09	BAK08	BAK07	BAK50	BAK51	BAK19
SiO ₂	62.39	64.28	58.86	59.12	60.22	60.68	61.42	61.72	61.91	61.91	61.91	60.19	60.31	60.34	62.11	62.52	62.64	62.71	62.82	67.25	72.01	75.06
TiO ₂	0.49	0.52	0.81	0.80	0.74	0.65	0.67	0.64	0.63	0.63	0.63	0.84	0.56	0.83	0.60	0.55	0.57	0.57	0.56	0.39	0.19	0.09
Al ₂ O ₃	17.36	17.02	17.08	16.79	17.09	16.74	17.15	16.83	16.54	16.54	16.54	17.43	18.19	17.40	17.57	17.34	17.49	17.56	17.53	16.34	15.16	14.33
Fe ₂ O ₃	2.28	1.62	1.40	1.41	1.47	1.39	1.80	1.26	1.22	1.22	1.22	1.93	1.72	2.00	1.67	1.81	1.63	1.67	1.46	1.04	0.47	0.24
FeO	2.55	1.95	4.51	4.43	4.04	3.89	3.71	3.74	3.63	3.63	3.63	3.46	1.86	3.49	2.94	2.50	2.86	2.76	2.90	1.89	0.99	0.71
MnO	0.13	0.10	0.11	0.11	0.10	0.10	0.11	0.09	0.09	0.09	0.09	0.11	0.09	0.11	0.11	0.10	0.11	0.11	0.10	0.05	0.15	0.10
MgO	1.90	1.13	3.51	3.67	3.32	3.36	3.51	2.90	2.85	2.85	2.85	2.15	1.39	2.11	1.62	1.45	1.54	1.48	1.48	1.49	0.48	0.25
CaO	5.09	3.88	6.34	6.47	6.06	5.95	6.12	5.63	5.48	5.48	5.48	5.41	4.09	5.33	5.00	4.71	4.87	4.86	4.87	3.93	1.61	1.29
Na ₂ O	4.18	4.79	3.78	3.76	3.89	3.95	4.00	3.98	3.85	3.85	3.85	4.39	4.48	4.48	4.44	4.38	4.42	4.38	4.53	4.62	5.07	4.43
K ₂ O	1.59	2.10	1.46	1.45	1.57	1.44	1.44	1.56	1.59	1.59	1.59	1.71	1.85	1.77	1.87	1.92	1.90	1.90	1.90	1.54	2.35	3.00
P ₂ O ₅	0.23	0.24	0.21	0.21	0.17	0.18	0.20	0.16	0.16	0.16	0.16	0.27	0.24	0.34	0.26	0.26	0.26	0.26	0.26	0.12	0.14	0.07
LOI	0.42	1.28	0.78	0.77	0.31	0.61	0.54	0.46	0.60	0.60	0.60	0.87	0.43	0.46	0.49	1.07	0.46	0.64	0.82	0.23	0.44	0.86
Total	98.61	98.90	98.84	98.98	98.97	98.95	100.66	98.95	98.54	98.54	98.54	98.74	95.30	98.65	98.66	98.60	98.74	98.90	99.23	98.89	99.06	100.44
Li	15.3	18.7	12.2	13.1	13.0	13.0	16.42	14.5	14.5	14.5	14.5	15.8	15.8	16.0	16.4	17.8	17.5	17.4	17.4	12.7	22.6	27.4
Be	1.14	1.37	0.88	0.88	0.80	0.80	1.20	0.79	0.79	0.79	0.79	1.20	1.28	1.28	1.12	1.11	1.14	1.11	1.11	0.93	1.70	1.50
Sc	7	5	16	16	20	13	16	18	14	14	14	8	10	13	8	5	11	8	7	8	3	4
V	78	56	172	172	157	139	143	137	137	137	137	128	70	125	78	66	73	72	72	71	7	5
Cr	11	8	49	68	48	72	67	52	53	53	53	13	12	13	14	9	15	8	10	22	11	14
Co	5	3	22	20	18	17	18	18	16	16	16	13	8	14	11	5	8	11	10	6	3	0
Ni	0	0	17	23	17	24	31	20	20	20	20	0	0	5	0	0	0	0	3	10	0	0
Cu	12	7	47	34	35	35	62	55	35	35	35	22	12	12	14	10	14	14	11	45	17	2
Zn	64	65	60	62	57	59	62	55	53	53	53	67	54	73	65	61	65	65	63	42	58	34
Ga	17	17	22	19	17	20	16	16	17	17	17	24	19	18	17	17	18	17	32	17	24	15
Rb	28	42	33	31	33	38	23	35	33	33	33	34	37	35	44	41	34	18	49	34	47	68
Sr	492	540	480	478	456	471	465	482	446	446	446	525	518	589	506	487	506	495	498	655	324	213
Y	7	26	18	8	16	27	2	9	30	30	30	0	18	14	25	12	20	5	35	2	11	12
Zr	126	149	117	118	113	117	123	112	112	112	112	137	127	138	129	137	134	136	130	87	125	68
Nb	4.1	5.8	3.5	3.5	2.8	2.8	4.8	2.8	2.8	2.8	2.8	4.8	5.4	5.4	4.3	4.4	4.3	4.3	4.3	1.9	6.4	5.5
Cs	0.89	1.53	0.80	0.80	0.76	0.76	0.93	0.93	0.93	0.93	0.93	1.18	1.25	1.25	1.16	1.13	1.14	1.09	1.09	0.29	1.44	2.15
Ba	525	657	454	461	449	449	465	483	503	503	503	528	572	551	585	616	599	602	602	563	787	859
La	14.4	19.2	12.0	12.0	11.4	11.4	14.9	14.9	12.0	12.0	12.0	14.9	17.1	17.1	15.1	15.8	15.3	15.4	15.4	10.9	14.5	14.5
Ce	31.6	41.4	26.4	26.5	24.6	24.6	34.1	25.6	25.6	25.6	25.6	34.1	38.4	38.4	32.7	34.0	33.0	33.0	33.0	22.6	31.7	29.1
Pr	4.2	5.4	3.6	3.6	3.4	3.4	4.7	3.4	3.4	3.4	3.4	4.7	5.3	5.3	4.4	4.5	4.4	4.4	4.4	2.9	4.3	3.8
Nd	16.7	20.9	15.1	15.1	13.7	13.7	19.5	13.6	13.6	13.6	13.6	19.5	21.9	21.9	17.6	18.3	18.0	17.9	17.9	11.4	16.0	13.0
Sm	3.5	4.2	3.4	3.4	3.0	3.0	4.4	3.0	3.0	3.0	3.0	4.4	4.9	4.9	3.7	3.8	3.8	3.8	3.8	2.3	3.1	2.4
Eu	1.05	1.16	1.02	1.01	0.93	0.93	1.31	0.89	0.89	0.89	0.89	1.31	1.33	1.33	1.12	1.12	1.10	1.10	1.10	0.63	0.77	0.50
Gd	2.7	3.2	2.9	3.0	2.6	2.6	3.7	2.6	2.6	2.6	2.6	3.7	3.9	3.9	3.1	3.2	3.0	3.0	3.0	1.8	2.2	1.7
Tb	0.44	0.48	0.45	0.46	0.40	0.40	0.57	0.38	0.38	0.38	0.38	0.57	0.58	0.58	0.48	0.50	0.48	0.47	0.47	0.26	0.35	0.27
Dy	2.4	2.7	2.6	2.6	2.3	2.3	3.1	2.3	2.3	2.3	2.3	3.1	3.2	3.2	2.8	2.7	2.7	2.8	2.8	1.4	2.0	1.5
Ho	0.49	0.50	0.52	0.52	0.47	0.47	0.61	0.46	0.46	0.46	0.46	0.61	0.62	0.62	0.53	0.55	0.55	0.55	0.55	0.26	0.41	0.28
Er	1.39	1.51	1.48	1.48	1.32	1.32	1.71	1.30	1.30	1.30	1.30	1.71	1.72	1.72	1.60	1.63	1.59	1.53	1.53	0.72	1.24	0.84
Tm	0.21	0.24	0.21	0.22	0.19	0.19	0.26	0.18	0.18	0.18	0.18	0.26	0.25	0.25	0.25	0.24	0.24	0.25	0.25	0.11	0.20	0.13
Yb	0.23	0.24	0.22	0.21	0.20	0.20	0.25	0.19	0.19	0.19	0.19	0.25	0.25	0.25	0.25	0.24	0.24	0.25	0.25	0.10	0.20	0.13
Lu	0.23	0.24	0.22	0.21	0.20	0.20	0.25	0.19	0.19	0.19	0.19	0.25	0.25	0.25	0.25	0.24	0.24	0.25	0.25	0.10	0.23	0.13
Hf	2.62	4.10	2.85	2.89	2.91	2.91	3.47	2.95	2.95	2.95	2.95	3.47	3.59	3.59	3.25	3.56	3.39	3.35	3.35	2.80	2.85	2.06
Ta	0.23	0.31	0.21	0.20	0.20	0.18	0.20	0.20	0.20	0.20	0.20	0.26	0.27	0.27	0.24	0.26	0.25	0.25	0.23	0.17	0.46	0.50
Tl	0.24	0.27	0.15	0.15	0.16	0.16	0.15	0.15	0.15	0.15	0.15	0.16	0.18	0.18	0.21	0.22	0.18	0.21	0.21	0.16	0.30	0.44
Pb	5.7	8.3	5.0	4.9	4.9	4.9	6.3	5.7	5.7	5.7	5.7	6.3	6.6	6.6	6.5	6.7	6.4	6.7	6.7	6.7	11.4	8.5
Th	2.19	3.57	1.91	1.86	2.04	2.04	2.60	1.98	1.98	1.98	1.98	2.60	2.77	2.77	2.67	2.87	2.80	2.64	2.64	2.13	2.08	3.28
U	0.95	1.52	0.93	0.98	0.88	0.88	1.15	1.06	1.06	1.06	1.06	1.15	1.23	1.23	1.29	1.36	1.33	1.33	1.33	0.98	1.23	2.05

Tab. 4-2 Sr-, Nd-, and Pb-isotope composition of Quaternary volcanics in the Bakening area

	$^{87}\text{Sr}/^{86}\text{Sr}$	$^{143}\text{Nd}/^{144}\text{Nd}$	$^{206}\text{Pb}/^{204}\text{Pb}$	$^{207}\text{Pb}/^{204}\text{Pb}$	$^{208}\text{Pb}/^{204}\text{Pb}$
Upper Quaternary basaltic rocks from monogenetic centers					
BAK04	0.70311	0.51307	18.347	15.492	38.015
BAK18	0.70317	0.51307			
BAK17	0.70315	0.51307	18.298	15.493	37.998
BAK24	0.70317	0.51306	18.345	15.501	38.062
BAK30	0.70327	0.51304			
BAK31	0.70329	0.51303	18.334	15.482	38.032
O26	0.70322	0.51307			
Lower Quaternary plateau basalt					
BAK06	0.70337	0.51303			
Upper Quaternary dacitic rocks					
BAK09	0.70329	0.51302	18.279	15.468	37.921
BAK10	0.70327	0.51304			
BAK39	0.70332	0.51306	18.281	15.472	37.924
Late Pleistocene thuja rhyodacite					
BAK19	0.70322	0.51308			

Tab. 4-3

REE-data of mineral separates of amphibole and plagioclase from the cumulate BAK63 (WR) determined by ICPMS (all values in ppm).

	amphibole	plagioclase	amph/WR	plag/WR
La	1.8	2.5	0,1	0.2
Ce	7.8	3.9	0,3	0.1
Pr	1.8	0.4	0.5	0.1
Nd	12.4	1.4	0.8	0.1
Sm	5.0	0.1	1.7	0.0
Eu	1.6	0,4	2.0	0.5
Gd	5.4	0.1	2.3	0.0
Tb	0.9	b.d.l.	2.7	
Dy	5.5	0.0	3.0	0.0
Ho	1.1	b.d.l.	2.9	
Er	2.9	b.d.l.	2.6	
Tm	0.4	b.d.l.	2.4	
Yb	2.3	b.d.l.	2.0	
Lu	0.3	b.d.l.	1.8	
Nb	1.1	b.d.l.	0.3	
Zr	43	1.0	0.4	0.0
Pb	2.9	1.3	0.5	0.2
Sr	265	1020	0.6	2.4
Ba	80	100	0.1	0.1

b.d.l. = below detection limit

Tab. 4-4

Last square calculation for the REE pattern of the dacitic rocks, using $D_{\text{mineral/melt}}$ values of Fujimaki, 1986 and Fujimaki et al., 1984. The best fit was found for fractionation of 20 % amph, 12 % plag, 7 % cpx and 0.6 % apatite. All concentrations in ppm.

	parent (BAK-42)	daughter (BAK-03)	calc. daughter
La	11.63	15.10	14.94
Ce	28.27	32.71	33.15
Pr	4.26	4.40	4.54
Nd	19.26	17.63	18.63
Sm	4.62	3.72	3.66
Eu	1.36	1.12	1.10
Gd	3.90	3.07	3.02
Tb	0.60	0.48	0.47
Dy	3.35	2.75	2.66
Ho	0.63	0.53	0.53
Er	1.83	1.60	1.65
Tm	0.26	0.25	0.24
Yb	1.72	1.62	1.63
Lu	0.25	0.25	0.25

References

- Ayers, J.C. and Eggler, D.H., 1995. Partitioning of elements between silicate melt and H₂O-NaCl fluids at 1.5 and 2.0 GPa pressure; implications for mantle metasomatism. *Geochimica et Cosmochimica Acta*, 59(20): 4237-4246.
- Bailey, J.C., 1996. Role of subducted sediments in the genesis of Kurile-Kamchatka island arc basalts; Sr isotopic and elemental evidence. *Geochemical Journal*, 30(5): 289-321.
- Brenan, J.M., Shaw, H.F. and Ryerson, F.J., 1995a. Experimental evidence for the origin of lead enrichment in convergent-margin magmas. *Nature (London)*, 378(6552): 54-56.
- Brenan, J.M., Shaw, H.F., Ryerson, F.J. and Phinney, D.L., 1995b. Mineral-aqueous fluid partitioning of trace elements at 900 degrees C and 2.0 GPa; constraints on the trace element chemistry of mantle and deep crustal fluids. *Geochimica et Cosmochimica Acta*, 59(16): 3331-3350.
- Churikova, T., Dorendorf, F., Wörner, G. and Eisenhauer, A., 2000. Across-Arc systematic geochemical zonation in trace elements and U/Th isotopes in Kamchatka reveal intra-arc rifting and its possible causes. (in prep.).
- Dirksen, O.V. and Melekestsev, I.V., 1998. Monogenetic volcanism at the vicinity of Bakening volcano (Kamchatka, Russia), Kamchatkan - Aleutian Workshop, July 1-9, 1998, Petropavlovsk/Kamchatsky, pp. 35-36.
- Ditmar, K.v., 1890. *Reisen und Aufenthalt in Kamtschatka in den Jahren 1851-1855. Erster Theil Beiträge zur Kenntnis des Russischen Reiches und der angrenzenden Länder Asiens*, St. Petersburg.
- Dunn, T. and Sen, C., 1994. Mineral/ matrix partition coefficients for orthopyroxene, plagioclase, and olivine in basaltic to andesitic systems; a combined analytical and experimental study. *Geochimica et Cosmochimica Acta*, 58(2): 717-733.
- Fujimaki, H., 1986. Partition coefficients of Hf, Zr, and REE between zircon, apatite, and liquid. *Contributions to Mineralogy and Petrology*, 94(1): 42-45.
- Fujimaki, H., Tatsumoto, M. and Aoki, K.i., 1984. Partition coefficients of Hf, Zr, and REE between phenocrysts and groundmasses. In: W.V. Boynton and G. Schubert (Editors), *Proceedings of the Fourteenth lunar and planetary science conference; Part 2. JGR. Journal of Geophysical Research. B. American Geophysical Union, Washington, DC, United States*, pp. 662-672.
- Hart, S.R. and Dunn, T., 1993. Experimental cpx/ melt partitioning of 24 trace elements. *Contributions to Mineralogy and Petrology*, 113(1): 1-8.
- Hofmann, A.W., 1988. Chemical differentiation of the Earth; the relationship between mantle, continental crust, and oceanic crust. In: E. Welin (Editor), *Isotope geochemistry; the Crafoord symposium. Earth and Planetary Science Letters. Elsevier, Amsterdam, Netherlands*, pp. 297-314.
- Irvine, T.N. and Baranger, W.R., 1971. A guide to the chemical classification of the common volcanic rocks. *Can. J. Earth Sci.*, 8: 523-547.
- Ito, E. and Stern, R.J., 1986. Oxygen- and strontium-isotopic investigations of subduction zone volcanism; the case of the Volcano Arc and the Marianas island arc. *Earth and Planetary Science Letters*, 76(3-4): 312-320.
- Kepezhinskas, P. and Defant, M.J., 1996. Contrasting styles of mantle metasomatism above subduction zones; constraints from ultramafic xenoliths in Kamchatka. In: G.E. Bebout, D.W. Scholl, S.H. Kirby and J.P. Platt (Editors), *Subduction top to bottom*.

- Geophysical Monograph. American Geophysical Union, Washington, DC, United States, pp. 307-314.
- Kepezhinskas, P. et al., 1997. Trace element and Sr-Nd-Pb isotopic constraints on a three-component model of Kamchatka Arc petrogenesis. *Geochimica et Cosmochimica Acta*, 61(3): 577-600.
- Kersting, A.B. and Arculus, R.J., 1995. Pb isotope composition of Klyuchevskoy Volcano, Kamchatka and North Pacific sediments; implications for magma genesis and crustal recycling in the Kamchatkan arc. *Earth and Planetary Science Letters*, 136(3-4): 133-148.
- Koloskov, A.V., N, V.O., Ponomarev, G.P. and Fedorov, P.I., 1997. Ultramafic xenoliths in island-arc volcanics of various geochemical type. *Petrology*, 5(5): 431-447.
- LaTourrette, T., Hervig, R.L. and Holloway, J.R., 1995. Trace element partitioning between amphibole, phlogopite, and basanite melt. *Earth and Planetary Science Letters*, 135(1-4): 13-30.
- Macdougall, J.D. and Lugmair, G.W., 1986. Sr and Nd isotopes in basalts from the East Pacific Rise; significance for mantle heterogeneity. *Earth and Planetary Science Letters*, 77(3-4): 273-284.
- Melekestsev, I.V., Dirksen, O.V. and Girina, O.A., 1998. Gigantskii eksplozivno-obvalnyi zirk i oblomnaya lavina na vulkane Bakening (Kamchatka, Rossija), translated title: A giant explosive-landslide cirque and a detritical avalanche on Bakening volcano, Kamchatka. *Vulkanologija i Seismologija*(3): 12-24.
- Miller, D.M., Goldstein, S.L. and Langmuir, C.H., 1994. Cerium/ lead and lead isotope ratios in arc magmas and the enrichment of lead in the continents. *Nature (London)*, 368(6471): 514-520.
- Piip, B.I., 1947. Marschrutnie geologitscheskie nabljudeniya na juge Kamchatki, translated title: Field-geological studies in South Kamchatka. *Trudy Kamchatskoi Vulkanologicheskoi Stantsij*, 3.
- Plank, T. and Langmuir, C.H., 1993. Tracing trace elements from sediment input to volcanic output at subduction zones. *Nature (London)*, 362(6422): 739-743.
- Sisson, T.W., 1994. Hornblende-melt trace element partitioning measured by ion microprobe. In: S.F. Foley and S.R. van der Laan (Editors), *Trace-element partitioning with application to magmatic processes*. Chemical Geology. Elsevier, Amsterdam, Netherlands, pp. 331-344.
- Svjatlovsky, A.E., 1956. Istorija nowejshogo vulkanizma i obrasovanija reliefa v raione vulkana Bakenin, translated title: History of Recent volcanism in the area of the Bakening volcano. *Trudy laboratorii vulkanologii*, 12.
- Tatsumi, Y. and Eggins, S., 1995. Subduction zone magmatism. *Frontiers in earth sciences*. Blackwell Science, Cambridge, 211 pp.
- Todt, W., Cliff, R.A., Hanser, A. and Hofmann, A.W., 1984. ^{202}Pb - ^{205}Pb spike for Pb isotope analysis. *Terra Cognita*, 4: 209.
- Turner, S.P., McDermott, F., Hawkesworth, C.J. and Kepezhinskas, P., 1995. A U-series study of Kamchatka volcanics; constraints on source composition and melting conditions. In: Anonymous (Editor), *AGU 1995 fall meeting*. Eos, Transactions, American Geophysical Union. American Geophysical Union, Washington, DC, United States, pp. 537.
- Volynets, O.N., 1994. Geochemical types, petrology, and genesis of late Cenozoic volcanic rocks from the Kurile-Kamchatka island-arc system. *International Geology Review*, 36(4): 373-405.

- Volynets, O.N., Karpenko, S.F., Kay, R.W. and Gorrington, M, 1997. Isotopic composition of Late Neogene K-Na alkaline basalts of Eastern Kamchatka: Indicators of the heterogeneity of the mantle magma sources. *Geochemistry International*, 35: 884-896.
- White, W.M., Hofmann, A.W. and Puchelt, H., 1987. Isotope geochemistry of Pacific mid-ocean ridge basalt. *Journal of Geophysical Research, B, Solid Earth and Planets*, 92(6): 4881-4893.
- Zjurupa, A.I., 1978. Eroziionnaya kal'tsera vulkana Bakening (analiz kontseptsii genezisa)
Translated Title: Erosion of the Bakening Caldera; a conceptual analysis of its genesis.
Byulleten' Vulkanologicheskikh Stantsij, 54: 68-74.

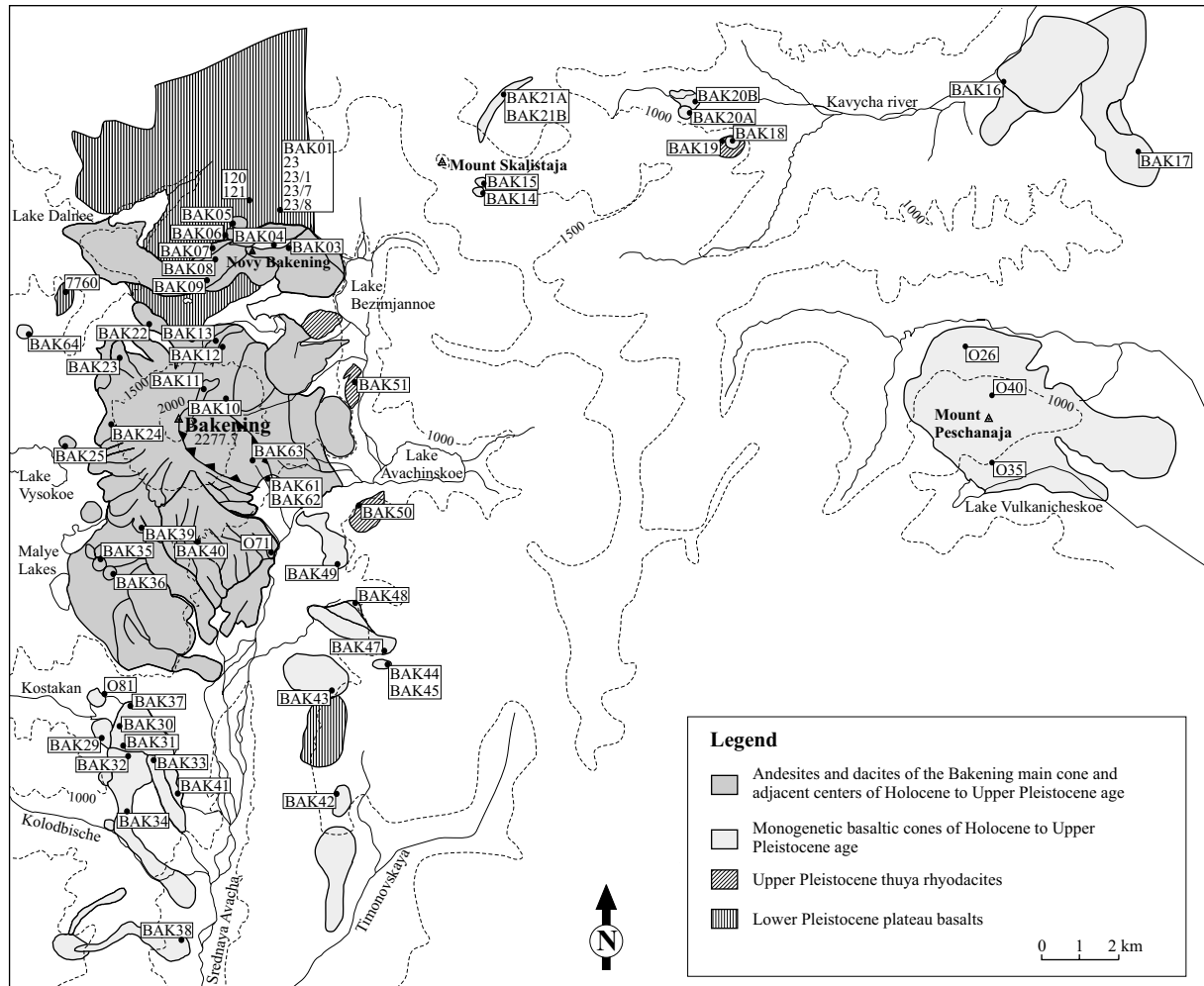


Fig. 4-1

Geological map of the Bakening volcano and the surroundings based on the field study in 1995 and 1996 and an unpublished map of I. Melekestsev.

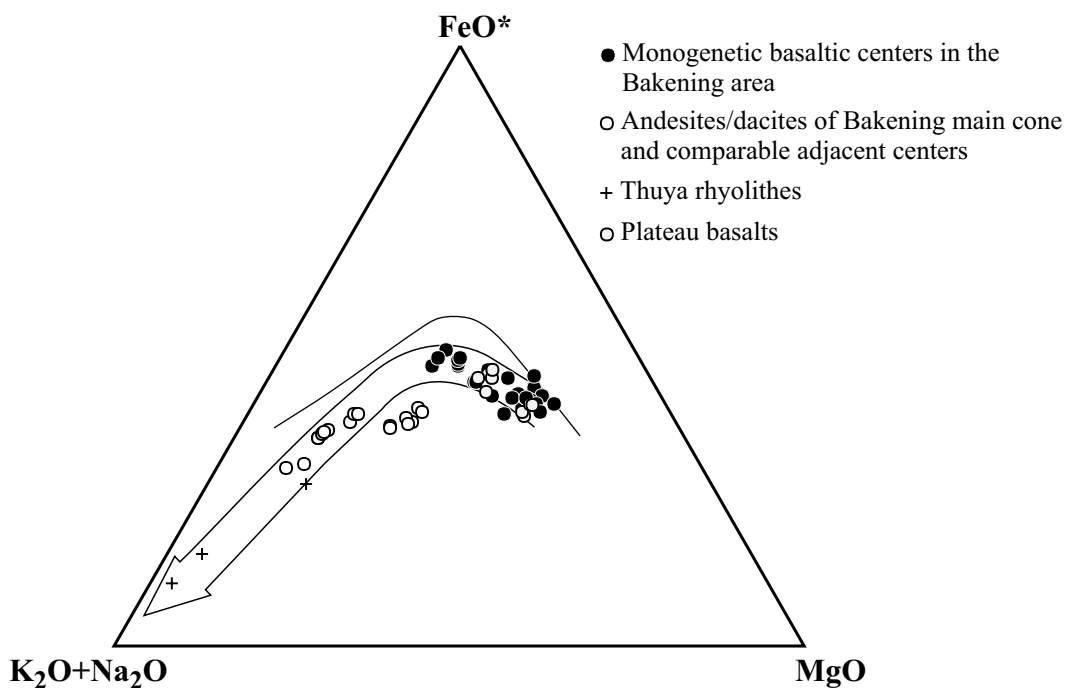
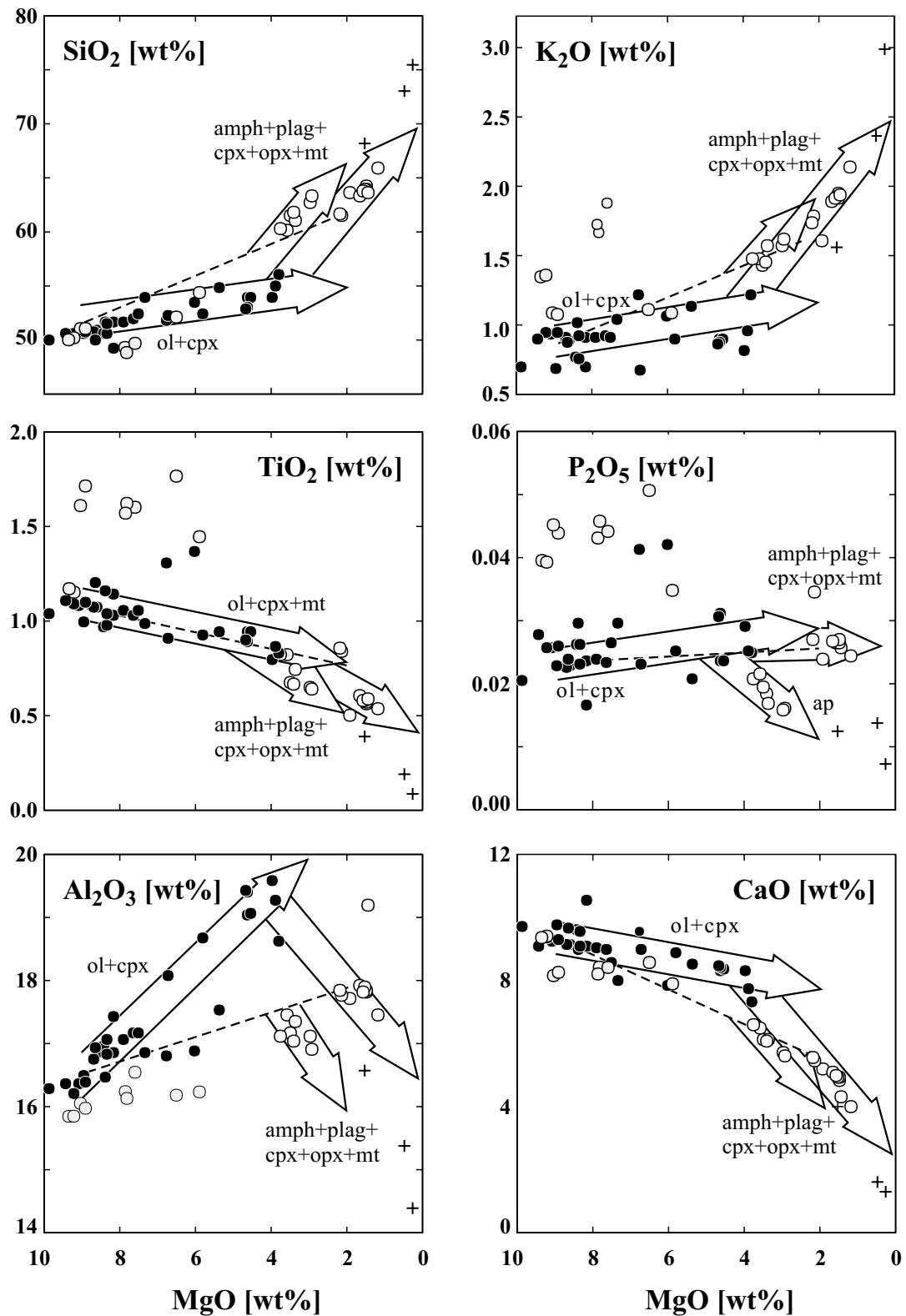
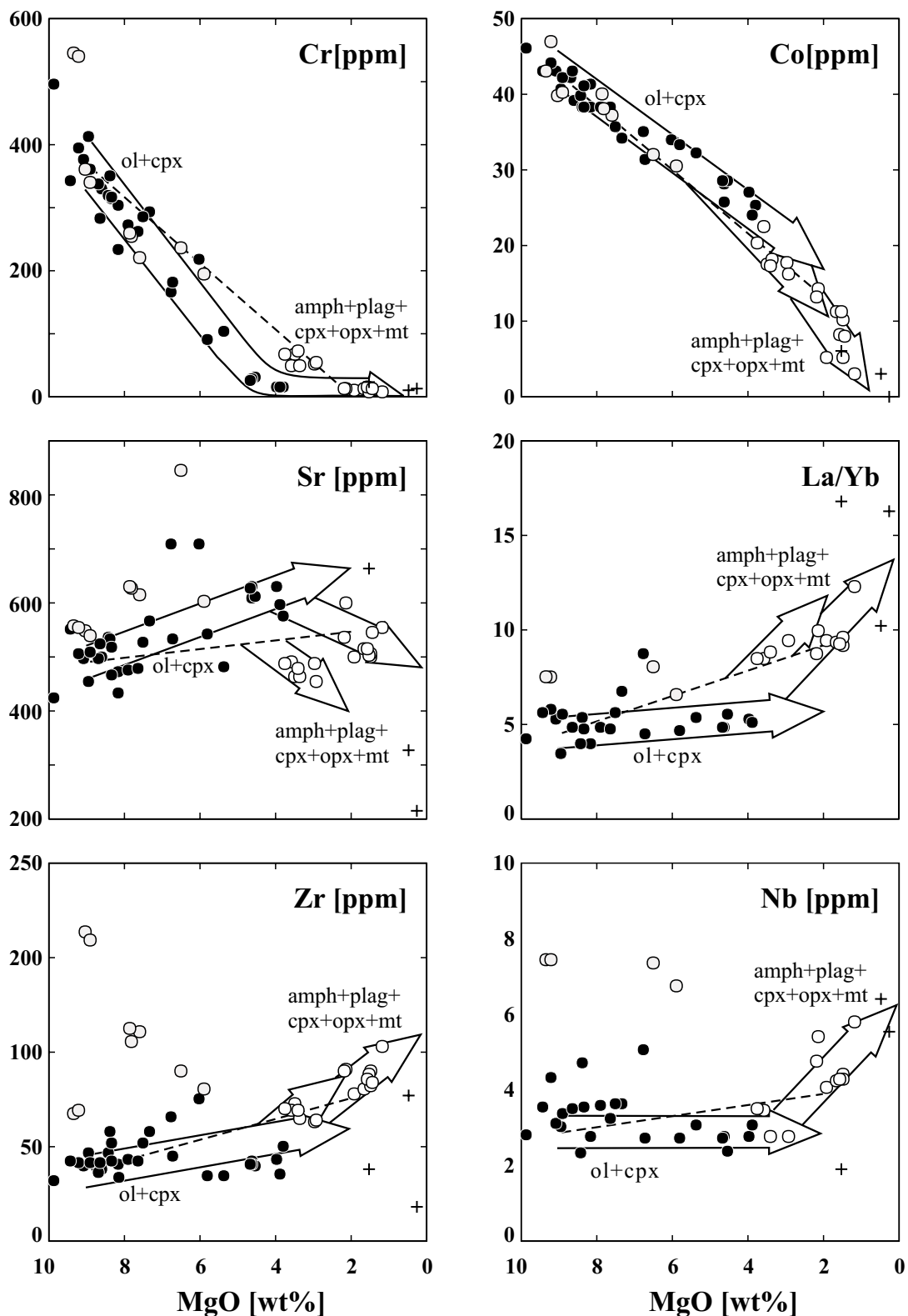


Fig. 4-2

AFM diagram, showing the lava compositions of the different Quaternary rock types at Bakening area. All studied rocks fall into the calc-alkaline field (boundary after Irvine and Baranger, 1971). The trends in the plateau basalts and Late Quaternary monogenetic basaltic centers follow the same trend. The dacitic and rhyodacitic samples are separated from the basaltic rocks and show a much different trend of strong Fe and Mg depletion, which is caused by the different fractionation assemblage in the two suites.

**Fig. 4-3**

Bivariate plots of major elements versus MgO. Symbols were used like in Fig. 4-2. The different trends in the Upper Quaternary basaltic and dacitic rocks are caused by a variable mineral fractionation, which is emphasized by the arrows. The Plateau basalts are displaced in most diagrams from these trends. Some dacitic rocks are obviously affected by mixing, which is outlined by the dashed line.

**Fig. 4-4**

Bivariate plots of trace elements versus MgO. Same symbols like in Fig. 4-2. Similar to major elements the different fractionating phases cause the different trends in the basaltic and dacitic rocks. Fractionation trends are stressed by arrows, the mixing between basaltic and dacitic melts outlined by a dashed line. Again plateau basalts are distinct from the Upper Quaternary basaltic rocks.

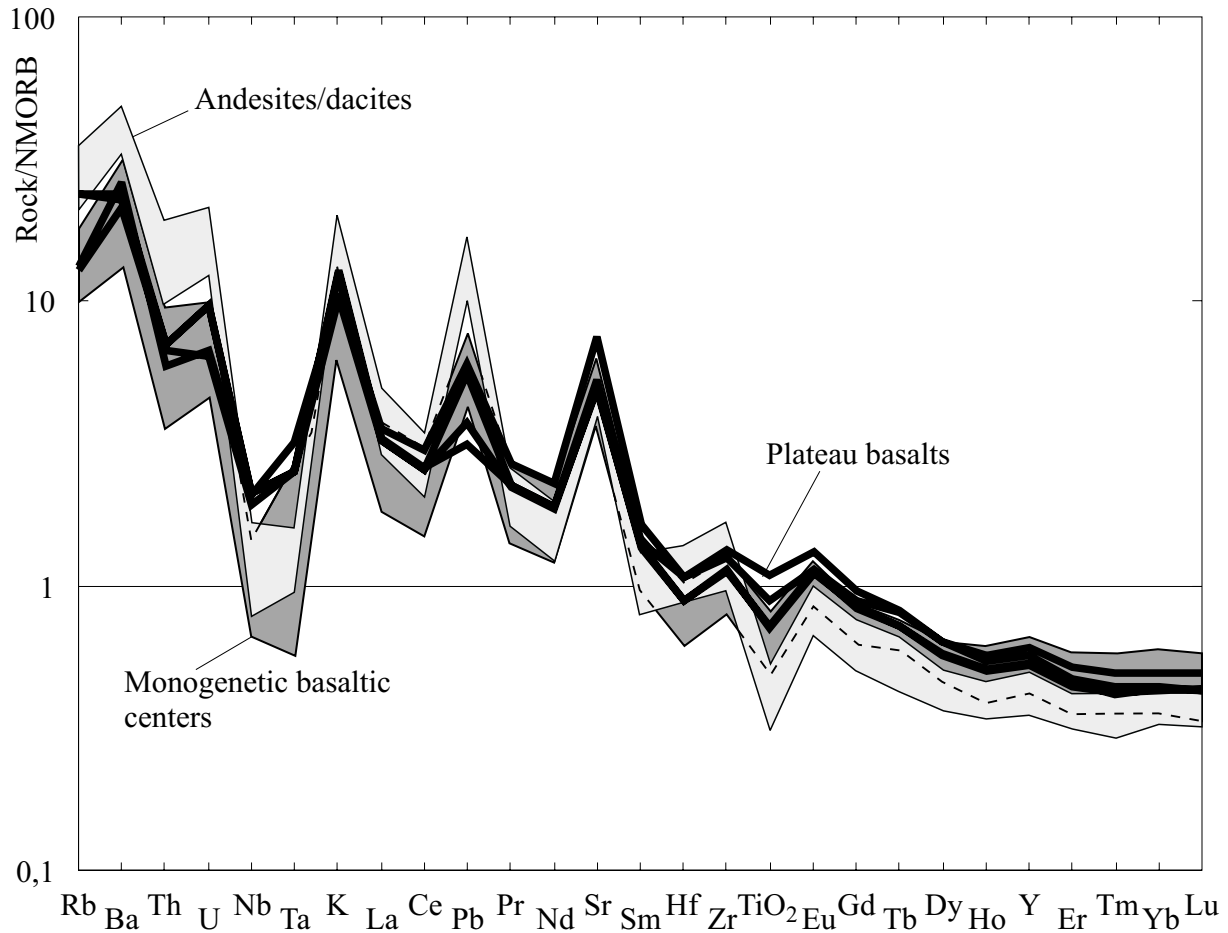


Fig. 4-5

Spider diagram, showing the trace element variation in the volcanic rocks of the Bakening area. For clarity, the Upper Quaternary basaltic and dacitic rocks are only expressed by compositional fields, which are based on 28 and 12 analyses, respectively. Analyses of plateau basalts were added for comparison. The normalization values for NMORB and the element order are those from Hofmann (1988). The Late Quaternary rocks are expressed by compositional fields. Remarkable is the general similar pattern of all three groups. In detail however, dacitic rocks display higher concentrations in the very incompatible elements but lower concentrations in HREE than the basaltic rocks. Plateau basalts differ by the less pronounced depletion in HFS elements from the Upper Quaternary rocks.

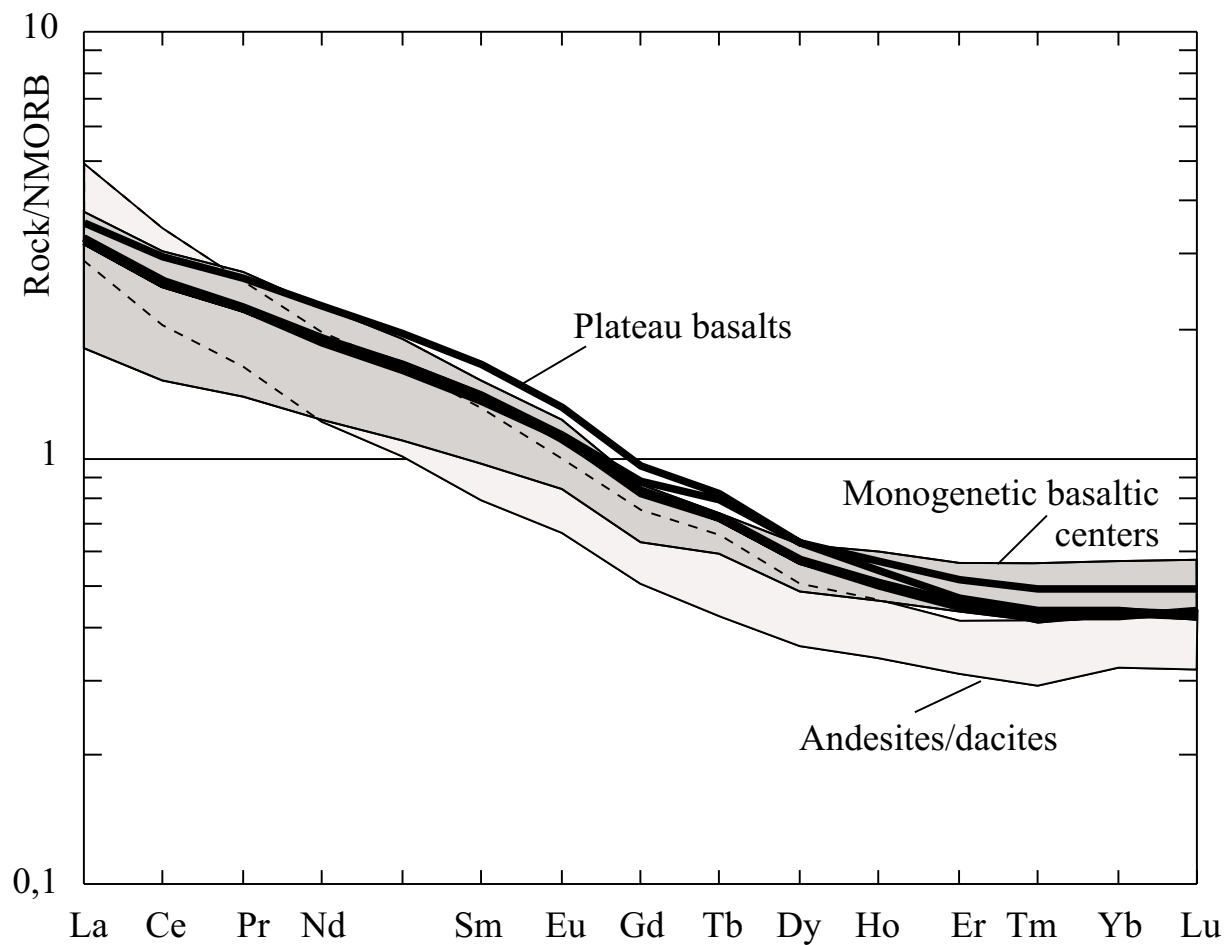


Fig. 4-6

Diagram, showing the REE variation in the rocks of the Bakening area. The normalization values for NMORB are those from Hofmann (1988). All suites have comparable depleted HREE and enriched LREE concentrations compared to NMORB. Plateau basalts have steeper pattern than the younger basaltic rocks. The dacitic rocks are most HREE depleted and LREE enriched, resulting in the cross-over of the pattern.

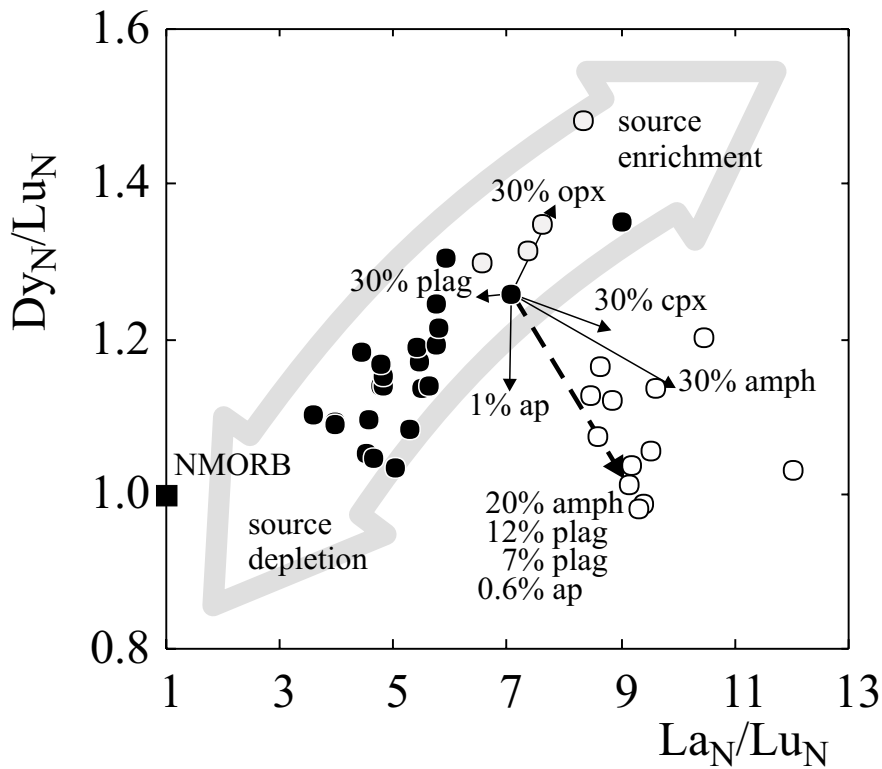


Fig. 4-7

Plot of NMORB normalized ratios of La/Lu versus Dy/Lu to distinguish between fractionation and melting processes, which influence the REE pattern. All samples are displaced to considerable higher La/Lu ratios compared to MORB, which can be explained by the slab fluid enrichment. The positive trend in the basaltic samples, including plateau basalts is caused by mixing between depleted and enriched mantle units. The dacitic samples are strongly influenced by mineral fractionation. Vectors for the different phases and the calculated fractionation assemblage are shown. These vectors are only applicable for the dacitic samples. The fractionation of cpx, amph, ol, and plag has a neglectable effect in basaltic rocks, because of the much lower mineral/melt partition coefficients. Normalization on NMORB after Hofmann (1988).

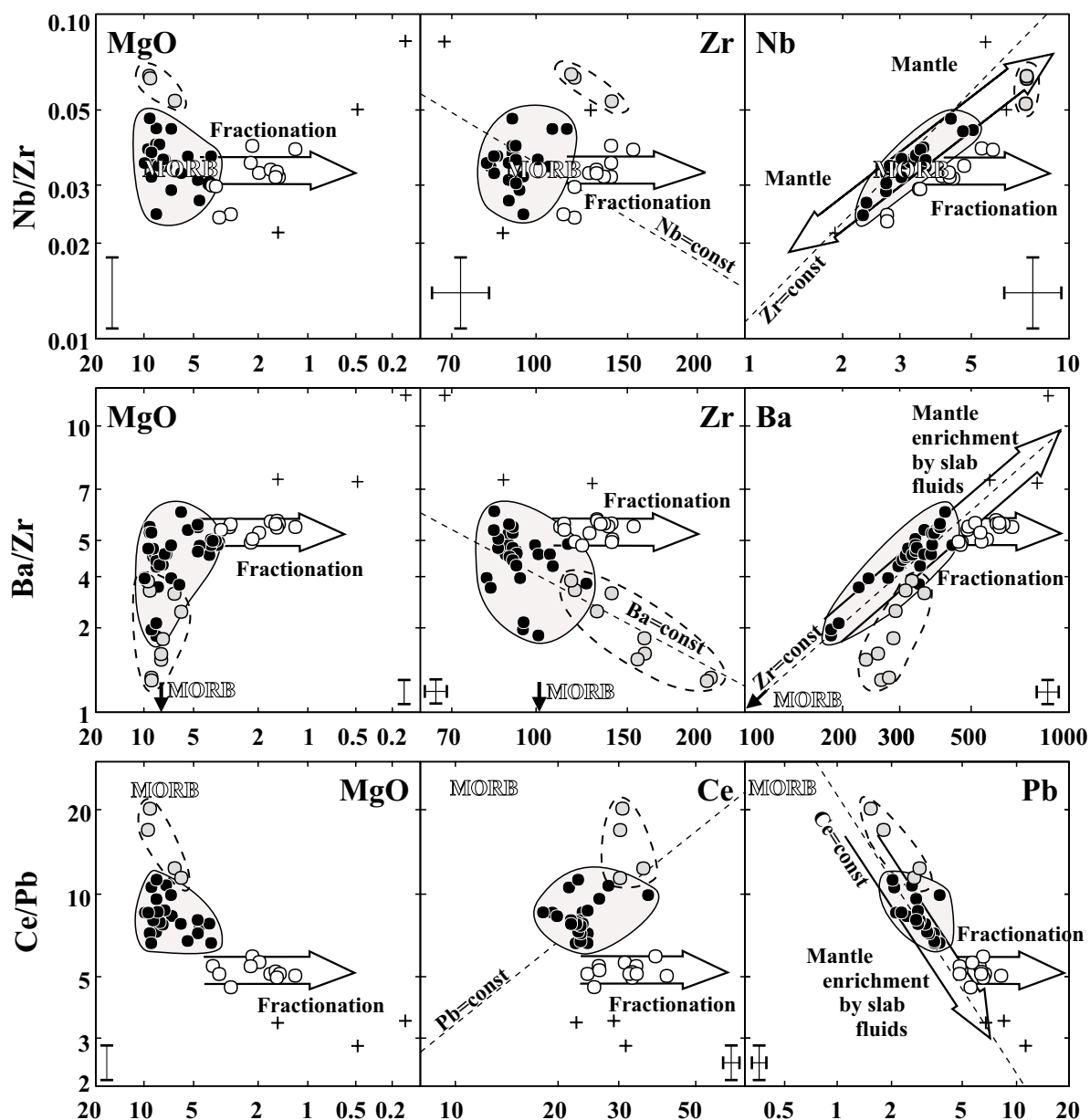


Fig. 4-8

Incompatible trace element ratios, used to distinguish between source depletion and enrichment processes. The ratio is always used for the y-axis. MgO and both incompatible elements for the x-axis are used as fractionation index. Fractionation or different mantle melting should result in horizontal trends. Any correlations therefore have to be caused by variable source compositions. The reasons are discussed in the text.

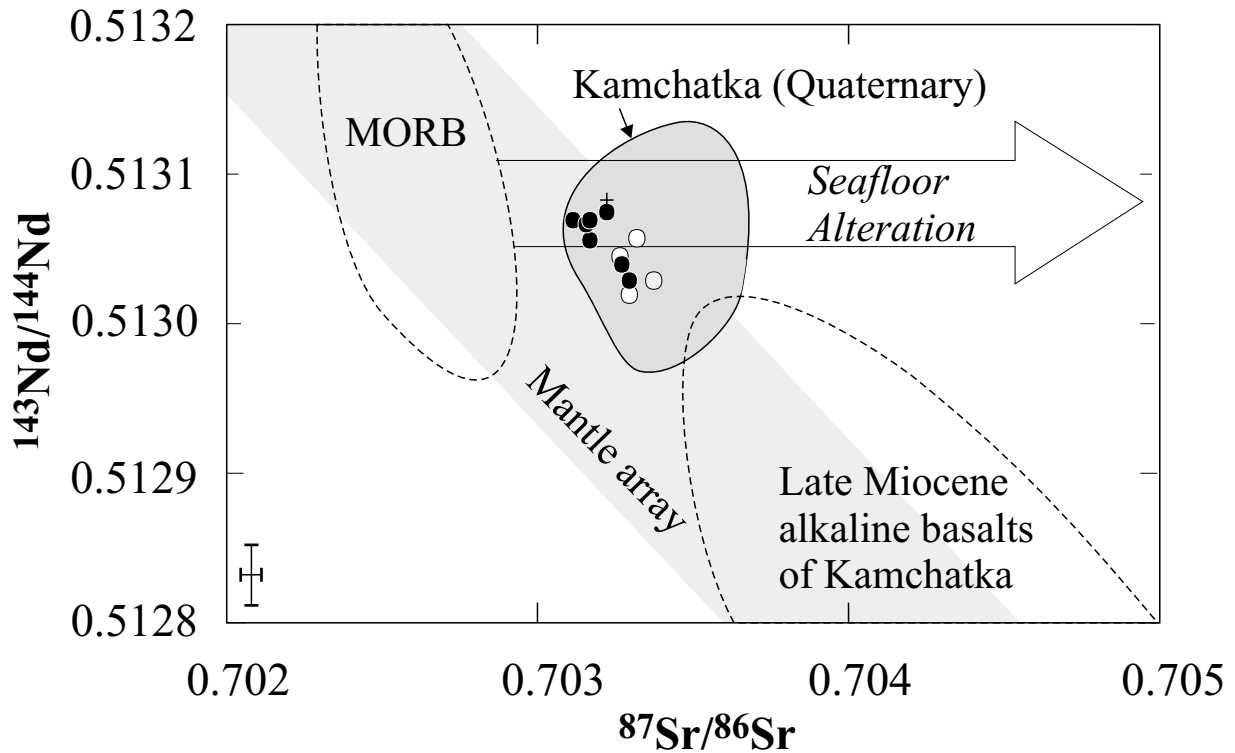


Fig. 4-9

Sr and Nd isotopes of rocks from the Bakening area. The MORB field (Ito and Stern, 1986; Macdougall and Lugmair, 1986; White et al., 1987) and the field for Miocene alkali basalts (Volynets et al., 1997) are added for comparison. The values for Bakening are very primitive and show not much variations. The slight displacement from the mantle array to a more radiogenic Sr-isotopic composition is caused by slab fluids, derived from the altered oceanic crust. Such seafloor alteration change the Sr-isotopic ratios but has no influence on Nd. Same symbols like in Fig. 4-2.